ISSN 1669- 3264

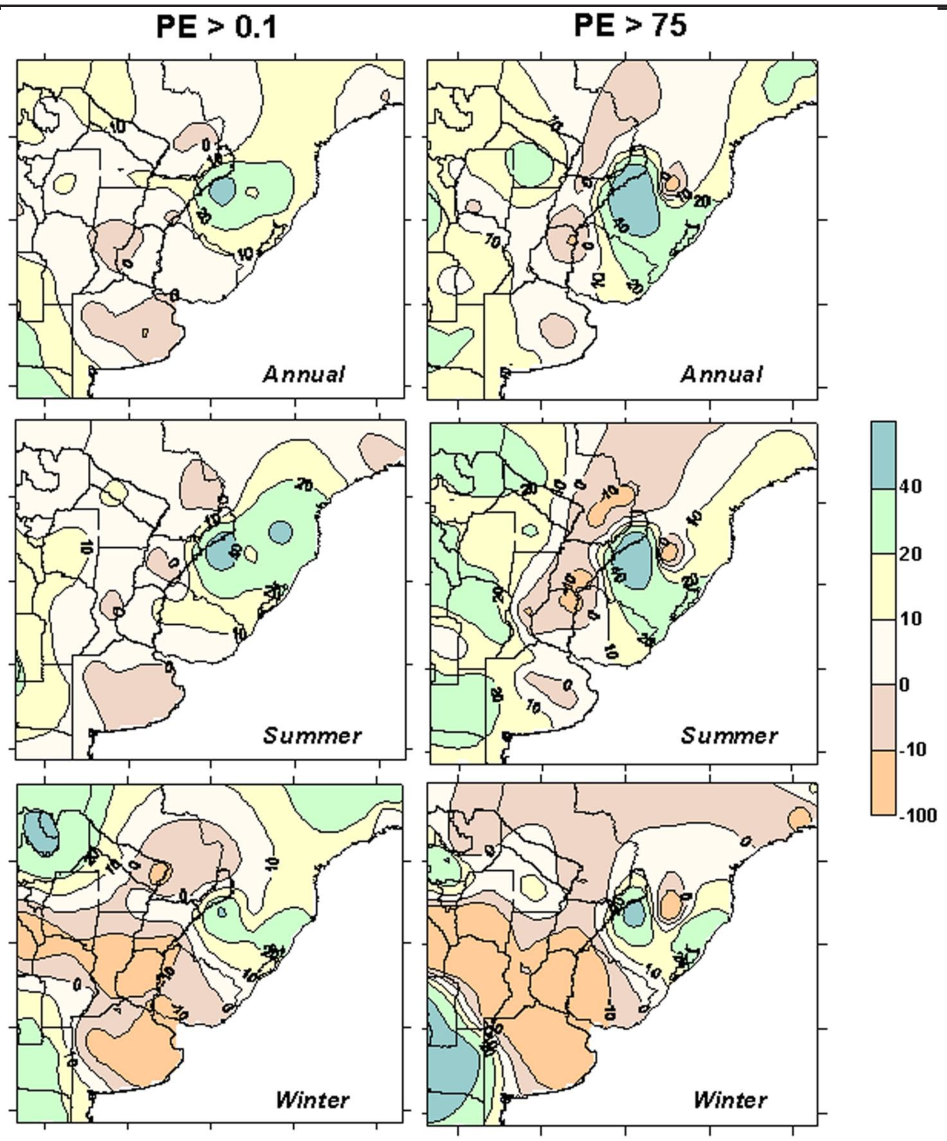

Figure 7: Percentage change for PE>0.1(left) and PE>75th (right) for annual, summer and winter values
(See article on page 13)

CLARIS NEWS

The Newsletter of the **European Project of the 6th Framework programme**

A Europe-South America Network for Climate Change Assessment and Impact Studies

Issue 5 - December 2006

The CLARIS Project is coordinated by CNRS CENTRE NATIONAL DE LA RECHERCHE SCIENTIFIQUE

EDITORIAL

Dear Colleagues,

In January 2007, the CLARIS project will enter its last six months of existence. Although much is still to come during this period, I want to thank you all for your dedication to the project and for allowing us all to reach common objectives. I believe that, in addition to the scientific achievements, among our major results are the new collaborations, which were developed between partners who did not know each other before, or the ones, which were strengthened thanks to the project framework.

During the coming months, we will have the opportunity to give the CLARIS network a new dynamics and set of objectives by responding to the European Commission call on the past and future climate of the La Plata Basin and its impacts on society. This new challenge is only possible thanks to the creation of the CLARIS network and its achievements acknowledged by the European Commission. And I thank you in advance for your support and future contribution to this new project.

I wish you all a Happy New Year 2007.

Jean-Philippe Boulanger

CLIMATOLOGY OF 1000 HPA WEATHER TYPE CIRCULATIONS IN SOUTHERN SOUTH AMERICA. ASSOCIATION WITH RAINFALL EPISODES

M. Laura Bettolli[#], Olga C. Penalba[*] and Walter M. Vargas[* #]*

1. INTRODUCTION

Climate variations have significant economic and social consequences, particularly in regions with agricultural production of worldwide importance. The study of climate variability in terms of the characterization of atmospheric circulation and its relation with local climate is a useful tool for diagnostics and forecast. There are few studies where objective identification and classification of synoptic patterns in southern South America has been performed. These topics have been widely discussed in the Northern Hemisphere and other regions of the planet (Mo and Ghil, 1988; Michelangeli et al., 1995; Kidson, 2000, among others). However, as first approximations to objective synoptic classifications in southern South America, Compagnucci and Vargas (1985), Compagnucci and Salles (1997) and Compagnucci et al. (1998) identified the principal spatial patterns by means of principal component analysis of observed daily sea-level pressure. Solman and Menéndez (2003) classified winter daily fields of 500 hPa geopotential heights for the period 1966-1999 by means of K-means clustering technique and studied their relationship with precipitation and temperature in Argentina. Bischoff and Vargas (2003) studied the 500 and 1000 hPa weather type circulations and their relationship with some extreme climatic conditions using reanalyses developed by the ECWMF for the period 1980-1988.

* *Departamento de Ciencias de la Atmósfera y los Océanos, FCEN, UBA, Buenos Aires, Argentina*
# *Consejo Nacional de Investigaciones Científicas y Técnicas (CONICET)*

The aim of this work is to advance towards an objective identification of weather type circulations (WT) in the South American sector and analyze their main characteristics, frequency, distribution and temporal variability during the period when major precipitations in central-eastern Argentina occur (October to May). An objective classification of daily surface circulation fields is proposed by using a long database in order to relate these weather types to rainfall episodes in the argentine Pampas region.

Table 1. Frequency of occurrence and characteristics of the 1000 hPa WT

WT	Frequency	Description
WT1	15.4 %	Negative anomalies over the SW Atlantic. SW flow over the continent
WT2	16.4 %	Negative anomalies over the SE Pacific and positive anomalies over the SW Atlantic
WT3	13.9 %	Positive anomalies over the southern tip of the continent
WT4	10.9 %	Positive anomalies over the E of the continent
WT5	15.9 %	Positive anomalies over the SE Pacific and S of the continent and trough downstream
WT6	11.3 %	Negative anomalies centered at 45S-55W
WT7	16.2 %	Negative anomalies over the southern tip of the continent

2. DATA AND METHODOLOGY

Daily anomalies of 1000 hPa geopotential heights for the period 1979-2001 were used to perform the weather type (WT) classification. The series of 5346 daily maps was obtained from the NCEP Reanalysis 2 data provided by the NOAA-CIRES Climate Diagnostics Center. The months analyzed were those when major precipitations in central-eastern Argentina occurred (October

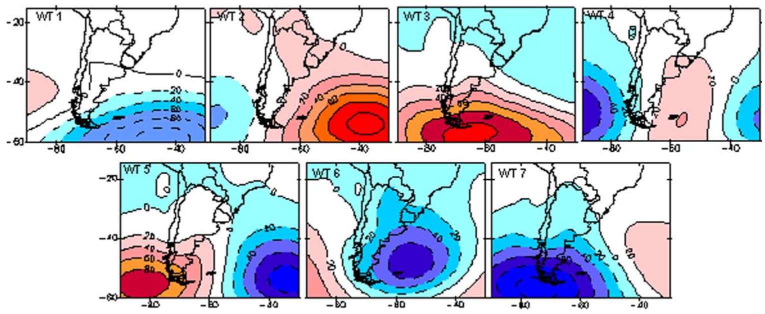

Figure 1. Spatial patterns of 1000 hPa WT

to May). This period also corresponds to the growing season of summer crops in this area. The domain chosen extends from 60°S to 20°S and from 90°W to 30°W including 475 gridpoints (2.5 x 2.5 latitude-longitude grid).

Principal component analysis (PCA) was performed (Richman, 1986; Jolliffe, 1986) coupled with cluster analysis (CA) (Wilks, 1995) to determine the weather types. PCA combined with CA classifies circulation patterns by performing cluster analysis in the daily loading for each principal component retained. The method of clustering used in this work is a K-means algorithm, which produces exactly K different clusters of greatest possible distinction with the goal to minimize variability within clusters and maximize variability between clusters. As shown by Gong and Richman (1995) this method combined with PCA can provide the most separable system of cluster.
High quality daily station datasets were used in this analysis in order to link the WT with the

regional climate. Although there are more raingauges in this region only 5 stations, obtained from the Argentine Meteorological, Service were deemed appropriate for the analysis with long records; less than 10% of missing data; and continuity of records. The used stations were: Paraná Aero (31°47’S; 60°29’W), Marcos Juárez Aero (32°42’S; 62°9’W), Rosario Aero (32°55’S; 60°47’W), Junín Aero (34°33’S; 60°55’W) and 9 de Julio (35°27’S; 60°53’W). The analyzed period was coincident with the one of reanalysis. The restrictive criterion used in this work to characterize days as a function of rainfall was based on Bettolli et al. (2005): a) rainy days: days with rainfall exceeding 0.1 mm in all stations b) heavy rainy days: days with rainfall exceeding 10 mm in all stations; c) dry days: days with no rainfall over the whole area.

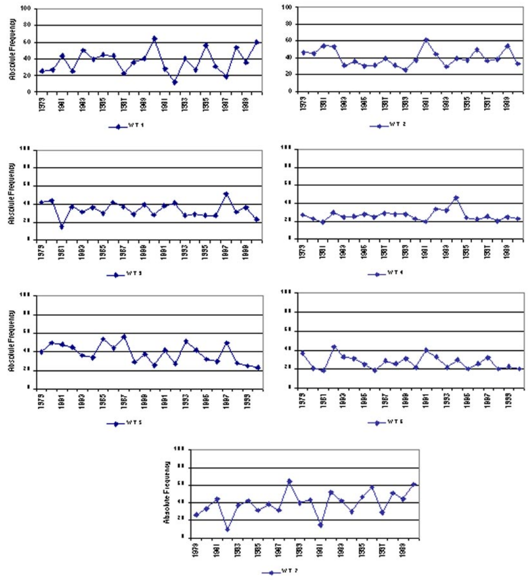

Figure 2. Time series of the number of occurrences per period (Oct to May). Each period is indicated by the initial year.

3. RESULTS

3.1 Weather Patterns

Using k-means clustering method on the most relevant T-mode principal components, a classification into 7 fundamental circulations was obtained. Separation between the centers of two clusters can be measured by means of the correlation coefficient between them and it should not exceed a threshold taken as 0.36 (Mo and Ghil, 1988). For the 7 clusters found here, the highest correlation value found was 0.38, which is an acceptable threshold for separation considering the big number of pairs involved in the calculation (475 pairs). The WT spatial patterns are presented in Figure 1 and their characteristics are summarized in Table 1. WT2 and WT6 are the less frequent patterns although there is a little variation in group frequencies.

The temporal series of seasonal frequencies of the 7 synoptic patterns were studied to find main characteristics, even though the analyzed period in this paper is relatively short to infer temporal variability (Figure 2). Major interannual variabilities are found for those groups with enhanced westerlies (WT1 and WT7) while the opposite behavior is found for those days characterized by a ridge in the east of the continent (WT4) inducing stability at low levels and warm advection. The maximum in the temporal series of this group is found for the period 1994/95, and it is coincident with precipitations below normal during 1994 and the following drought in 1995 that affected a vast region of Argentina (Ales-

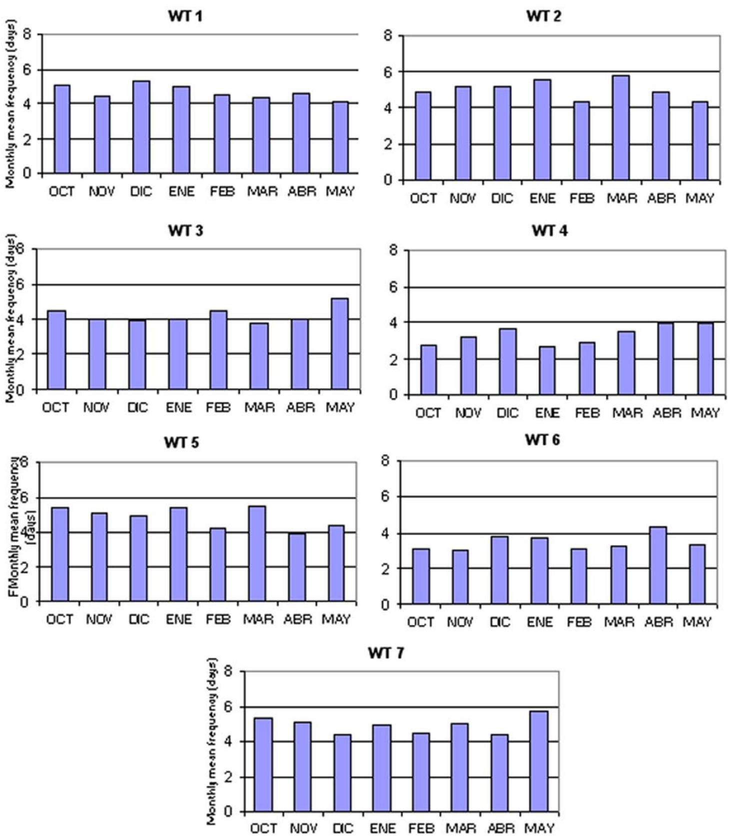

Figure 3. Monthly mean frequencies for each group of WT.

Table 2. Percentage of events of given duration (d) in days.

D	WT1	WT2	WT3	WT4	WT5	WT6	WT7
1	47.6	39.8	44.2	67.5	48.2	64.2	38.8
2	26.3	25.3	24.0	24.6	24.8	23.2	31.6
3	13.0	15.5	16.3	6.4	12.3	7.6	16.3
4	6.3	8.2	5.1	0.5	7.1	2.3	6.3
5	2.3	5.7	2.2	0.5	3.9	1.6	2.8
6	2.3	2.2	1.6	0.0	1.2	0.8	2.8
7	1.3	1.6	2.6	0.5	1.7	0.0	1.3
8	0.8	0.3	1.6		0.2	0.3	0.3
9	0.3	0.3	0.6		0.2		
10		0.5	0.6		0.2		
11		0.5	0.6				
12		0.5					
13							
14							
15			0.3				

sandro y Lichtenstein, 1996). A progressive diminution in time of cold air advection situations is observed (WT5) (significant linear trend at 5%) associated with an anticyclone which induces stability conditions at low levels. This result is coincident with the increase of summer minimum temperature values observed in recent decades over the studied area (Easterling et al., 1997; Rusticucci and Barrucand, 2004) which depend mainly on the night-time radiative effect. Meanwhile an increase in seasonal frequencies of enhanced mid-latitude westerlies and disturbance migration over Patagonia (WT7) is detected. This result is in agreement with the gradual increase in annual precipitation observed in recent decades over this area (Hoffmann et al. 1987; Castañeda and Barros 1994; Penalba and Vargas 1996). This group exhibits pronounced low frequencies in the strongest El Niño years (1982/83, 1991/92 and 1997/98) showing changes in low level circulation and in the intensity of westerlies during these years.

Monthly mean frequencies for each group are displayed in Figure 3. WT1 presents the highest frequencies in December in agreement with the maximum in the meridional circulation index which estimates the difference of 1000 hPa geopotential heights at 40°S between Pacific and Atlantic Oceans (Alessandro, 1998). This indicates an intense South Pacific high during this month. Situations with enhanced SE flow over central Argentina (WT3) reach their maximum during spring and fall. These situations can be associated with the SE windstorms (sudestadas) in the Rio de la Plata estuary and their monthly distribution is coincident with the results found by Ciappesoni and Salio (1997) and Escobar et al. (2004). WT6 presents maximum frequencies during April and summer months coinciding with Necco (1982) who found that oceanic cyclogenesis occurs most frequently during summer and transition seasons.

Not only the recurrence but also the persistence of anomalous conditions in circulation affects the local weather conditions. The persistence of each group was also analyzed (Table 2). The less persistent groups are WT4 and WT6 which represent opposite situations from the dynamical point of view (positive and negative anomalies in the east of the continent respectively). WT2 and WT3, with positive anomalies of geopotential height at high latitudes, are the most persistent patterns. WT7 presents 54% of its sequences in short duration (between 2

Table 3. Z test statistics. In brackets: relative difference with climatological frequency. Significant values at 95% (*) and at 90% (**).

WT	Dry Days	Rainy Days	Heavy Rainy Days
WT1	3.78* (13.2)	-3.24* (-31.1)	-0.09 (-2.3)
WT2	1.74** (6)	0.12 (1.3)	-0.09 (-2.4)
WT3	-3.97* (-14.7)	2.95* (39.3)	0.96 (30.3)
WT4	3.41* (13.9)	-1.87** (-22)	-0.60 (-17.4)
WT5	-2.76* (-9.6)	-1.76** (-17.8)	-1.36 (-30.6)
WT6	-3.98* (-16.1)	1.04 (14.1)	0.47 (15.6)
WT7	0.52 (1.8)	-0.50 (-5.3)	1.21 (36.2)

and 4 days).

3.2 Association with rainfall episodes

At this point, the objective is to find the main spatial patterns under which significant daily rainfall, or no rainfall at all, tends to occur. In order to evaluate the link between the occurrence of a specific atmospheric pattern and rainfall, the Z test was applied (Infante Gil and Zárate de Lara, 1984). This test compares relative frequencies. In particular for this study, the difference between the probability of occurrence of a rainy day (heavy rainy day or dry day) given a specific pattern of WT and the climatological probability of a rainy day (heavy rainy day or dry day) was evaluated by means of the Z statistic. Z values and their significance are shown in Table 3. If Z value is positive (negative) and significant, the specific pattern of WT has (has not) significant contribution to the rainfall condition.

Groups WT1 and WT4 contribute to dry conditions over the region since they present positive and the most significant values for dry days and negative values for the other days with wet conditions. Situations with a ridge to the east of the continent (WT4) also inhibit local rainfall (not shown). Conversely, rainy days are mostly related to situations with E-SE advection over the Pampas region (WT3). These situations also present negative significant values of Z indicating that this pattern does not favor dry conditions. In a similar way, pattern WT6 presents a positive statistic (although not significant) for rainy days and a negative significant one for dry days. Even though heavy rainy days do not present significant values with any group, WT7 seems to be the pattern most associated with this wet condition. This result in addition with the increases in time of both precipitation over the region and WT7 frequencies reinforces the idea that low frequency changes in annual precipitation are accompanied by changes in circulation.

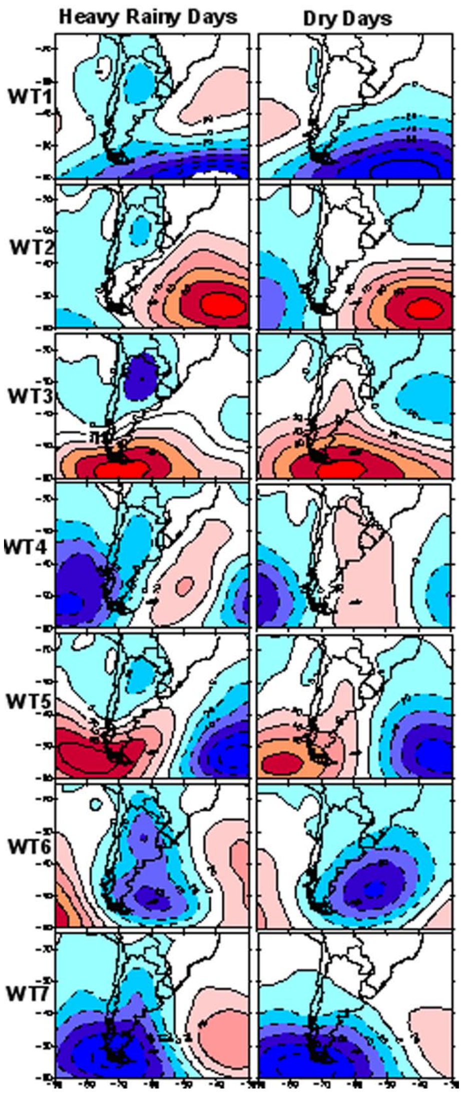

Figure 4. Composites of geopotential height anomalies for heavy rainy days (left panel) and dry days (right panel).

In order to analyze the circulation associated with rainy and dry episodes, heavy rainy days and dry days were kept and the composite fields of geopotential height anomalies were calculated for each condition of rainfall within each group. The composite patterns for the 7 groups are presented in Figure 4. In both cases (heavy rainy days and dry days), the spatial patterns respond to the large-scale spatial structure of the group they belong to, even though it can be observed lower scale anomalies that make the difference between both rainfall conditions. For heavy rainy days, each group presents cyclonic anomalies in central and northern Argentina. These patterns show

REFERENCES

Alessandro, A. P. and Lichtenstein, E. R., 1996: Situación sinóptica asociada a la Sequía del Invierno de 1995. Revista Geofísica, 45, 125-143.

Alessandro, A. P., 1998: Aspectos sinópticos de las intensas lluvias del verano 1982-1983 en el Sudeste de Sud América. Meteorologica, 23, 3-14.

Bettolli, M Laura; Penalba, Olga C. and Vargas, Walter M: Características de la precipitación diaria en la región núcleo sojera argentina. Proc. IX Congreso Argentino de Meteorología, Buenos Aires, Argentina, October 2005

Bischoff, SA and Vargas, WM, 2003: The 500 and 1000 hPa weather type circulations and their relationship with some extreme climatic conditions over southern South America. Int. J. Climatol., 23: 541-556

Castañeda, E. and Barros, V., 1994: Las tendencias de la precipitación en el Cono Sur de América al este de los Andes. Meteorologica, 19, 23-32.

Ciappesoni, H. and Salio, P., 1997: Pronóstico de Sudestadas en el Río de la Plata. Meteorologica, 22, 71-86.

Compagnucci, RH and Vargas, WM, 1985: Tipificación de los campos báricos de superficie para julio 1972-1977. Análisis por componentes principales no-rotadas. Geoacta, 13,1: 57-70

the biggest differences with each center of the group when it is compared with Figure 1. While spatial patterns associated with dry days show an enhanced anticyclonic anomaly over the region when this positive anomaly exists (as in WT3, WT4 and WT5) or the negative anomaly is reduced (as in WT1, WT6 and WT7).

4. CONCLUSIONS

This paper deals with synoptic situations represented by daily 1000 hPa geopotential fields in order to find synoptic patterns in southern South America. Principal component analysis was performed coupled with cluster analysis to determine the weather types. The seven outline spatial structures of WT obtained fit very well with the main synoptic fields recognized by forecasters.

The most outstanding results are: major interannual variabilities were found for those groups with enhanced westerlies (WT1 and WT7) while the opposite behavior was found for those days characterized by a ridge at the east of the continent (WT4) inducing subsidence at low levels and warm advection. It was observed a progressive diminution in time of cold air advection situations (WT5) associated with an anticyclone which induces stability conditions at low levels. This result is coincident with the increase of summer minimum temperature values observed in recent decades over the studied area which depend mainly on the night-time radiative effect. An increase in seasonal frequencies of enhanced mid-latitude westerlies and disturbance migration over Patagonia (WT7) was detected with minimum frequencies during El Niño years.

The analysis of the monthly frequencies for each group revealed that situations with negative anomalies over the SW Atlantic and SW flow over the continent (WT1) presented the highest frequencies in December in agreement with the maximum in the meridional circulation index (intense South Pacific high). Situations with SE flow over central Argentina (WT3) reach their maximum during spring and fall; this is coincident with the monthly distribution of the E-SE windstorm (sudestada) in the Rio de la Plata estuary. The more frequent oceanic cyclogenesis (WT6) occur during summer and transition seasons. The less persistent groups were WT4 and WT6 (positive and negative anomalies in the east of the continent respectively) which could be mostly related to short wave disturbances. WT2 and WT3 were the most persistent groups.

Wet (dry) conditions in the Pampas region are (are not) favored either by situations with positive anomalies over the southern tip of the continent probably associated to 'sudestadas' or by low centers in the Atlantic Ocean probably related to frontal passage or cyclogenesis. Heavy rainfall conditions are mostly related to situations with a disturbance in the north of Patagonia. Even though both heavy rainfall and dry patterns may belong to the same cluster, lower scale anomalies make the difference between both conditions. Heavy rainy days present cyclonic anomalies in central and northern Argentina and the biggest differences with each center of the group. On the contrary spatial patterns associated with dry days show an enhanced anticyclonic anomaly over the region or a reduced negative anomaly.

Although the spatial patterns found here constitute, of course, a simplification of the complex reality, they can be useful as additional objective elements for regional forecasters. That practicality may be increased in future studies in which other levels and variables could be taken into account.

Acknowledgments

This study was supported by grants from Universidad de Buenos Aires X234 and X135, from CONICET PIP 5139 and from GOCE-CT-2003-001454 CLARIS.

REFERENCES (cont.)

Compagnucci, RH and Salles, MA, 1997: Surface pressure patterns during the year over southern South America. Int. J. Climatol., 17: 635-653.

Compagnucci, RH and Vargas,WM, 1998: Inter-annual variability of the cuyo rivers' streamflow in the Argentinean Andean mountains and ENSO events. Int. J Climatol., 18: 1593-1609.

Easterling, D., Horton, B., Jones, P., Petterson, T., Karl, T., Parker, D., Salinger, M. J., Rasuvayev, V., Plummer, N., Jamason, P. & Folland, C., 1997: Maximum and minimum temperature trends for the globe. Science, 277, 364-367

Escobar, G., Vargas, W and Bischoff, S, 2004: Wind tides in the Rio de la Plata estuary: meteorological conditions. Int. J. Climatol., 24:1159-1169.

Gong, X. and Richman, M., 1995: On the Application of Cluster Analysis to Growing Season Precipitation Data in North America East of the Rockies. J. Clim: Vol. 8, No. 4, 897–931.

Hoffmann, J.A., Núñez S. and Gómez, A., 1987: Fluctuaciones de la precipitación en la Argentina, en lo que va del siglo. Proc. del II Congreso Interamericano de Meteorología. V Congreso Argentino de Meteorología, Buenos Aires, Argentina, 12.1.1-12.1.5

Infante Gil S, Zárate de Lara G. 1984: Métodos Estadísticos. Trillas: México; 643 pp

TEMPORAL VARIABILITY IN THE LENGTH OF NO-RAIN SPELLS IN ARGENTINA

Olga C. Penalba*, María P. Llano
Departamento de Ciencias de la Atmósfera y los Océanos
Facultad de Ciencias Exactas y Naturales
University of Buenos Aires, Argentina

1. INTRODUCTION

The analysis of daily rainfall in Argentina is a subject of great interest from the hydrological standpoint. This interest is not merely climatological; rainfall has to be considered in the design of hydrologic systems and the management of agricultural and natural resources. Central-north-eastern Argentina belongs to the La Plata Basin. Extreme events can cause enormous losses in the agricultural and cattle raising sector. In particular, changes in the probability of no rain spell would cause significant damage to agriculture and hydrology.
Precipitation in Argentina has strong geographical variations. These range from a very well defined annual cycle (peak rainfall during the warm season) in the north and northwest to an almost uniform distribution with small peaks during spring and autumn in the eastern-central area, northeastern Argentina to the scarce rainfall in the south (Rusticucci and Penalba, 2000; Penalba and Vargas, 2005). The daily rainfall regime and its geographic distribution over Argentina have been studied by Penalba and Robledo (2005). Daily precipitation percentiles and the frequency of rainday show the same spatial variation, with the greatest values in the northeast region.
The study of wet or dry spells for a significant number of stations is rather limited. Ruiz (2005) analyzed daily dry conditions in one station in Argentina; focusing on dry spells of 5 to 7 days. In the Argentine humid and semihumid region, Vargas and Alessandro (1985, 1990) estimated theoretically the sequences of temperature anomalies and monthly rainfall applying the geometrical distribution. Penalba and Vargas (2005) analyzed the spatial and temporal changes in the frequency of months per year of low rainfall and sequences of consecutive months with rainfall below normal and fitted them to two theoretical models, the binomial and the geometric in the Río de la Plata Basin.
Amongst the most frequently used stochastic procedures for the treatment of wet and dry spells are the Markov chains of different orders. Markov chains and their properties are used in many scientific fields (Haan et al. (1976), Moon et al. (1994), Gregory et al (1993), Martin-Vide and Gomez (1999), Tolika and Maheras (2005) and Lana and Burgueño (1998)).
The aim of this paper is to analyze the length of no-rain spells, the number of days comprising them and their temporal variability and in particular evaluate changes before and after the 1970's.

Figure 1: Distribution of the stations under study

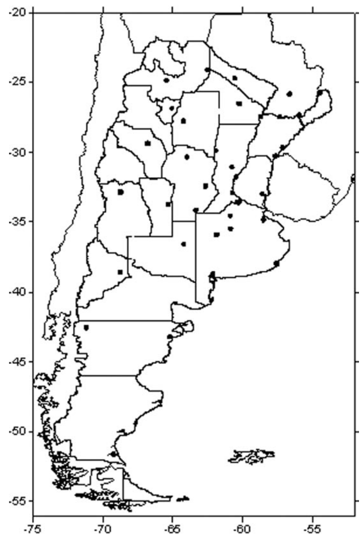

REFERENCES (cont. from page 7)
Jolliffe, I. T., 1986: Principal Component Analysis. Springer-Verlag. 271 pp.
Kidson JW, 2000: An analysis of New Zealand synoptic types. and their use in defining weather regimes. Int J Climatol. 20:299–316
Michelangeli, P. A., Vautard, R. and Legras, B., 1995. Weather Regimes: recurrence and quasistationarity. J. Atmos. Sci., 52:1237-1256.
Mo, K., and M. Ghil, 1988: Cluster analysis of multiple planetary flow regimes, J. Geophys. Res., 93D, 10927-10952.
Necco, G., 1982: Comportamiento de vórtices ciclónicos en el área Sudamericana durante el FGGE: Ciclogénesis. Meteorologica, XIII, 7-19.
Penalba O.C. and Vargas, W.M., 1996: Climatology of the extreme rainfall in Buenos Aires, Argentina, Meteorol. Appl., 3, 275-282.
Rusticucci, M.M. and Barrucand, M.G., 2004: Observed trends and changes in temperature extremes over Argentina. J. Clim. 17, 4099-4107.
Solman, SA and Menéndez, CG, 2003: Weather regimes in the South American sector and neighbouring oceans during winter. Climate Dynamics, 21, 1: 91-104.
Richman, M, 1986: Rotation of Principal Components. J. Climatol, 6, 293-335
Wilks D.F.,1995. Statistical Methods in the Atmospheric Sciences. Academic Press, 467 pp.

2. DATA AND METHODOLOGY

High quality daily station datasets are used in this analysis. Although there are more raingauges in Argentina only 35 raingauge stations and 1 Paraguayan station are deemed appropriate for the analysis of long records (more than 40 years). Records had less than 10% of missing data and continuity of records. All the information used in this study was supplied by the "Servicio Meteorológico Nacional" and the "Instituto Nacional de Tecnología Agropecuaria" (local organization). Data were processed to include the best available datasets: statistical tests, comparison with neighbouring stations and local knowledge (Sneyers, 1990). This database represents the different types of climates existing in Argentina, even though the number of raingauges with reliable daily data to the south of 40ºS (Patagonia region) and middle and high mountain areas (central-western region) is low (see Figure 1 for their locations).

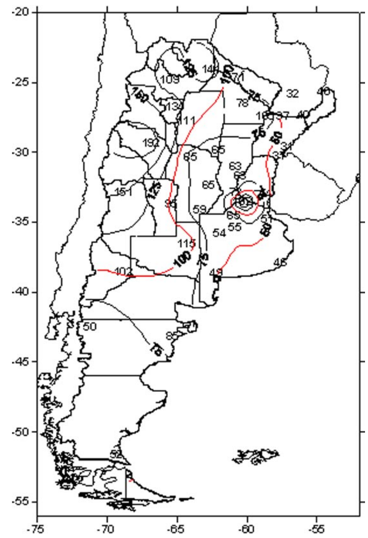

Figure 2: Maximum length in days of the dry spells

Precipitation events occurring on 29 February (leap year) were omitted. The shorter period analyzed was 1961-2003 and the longest one was 1911-2003.

The definition of no-rain spells is based on the length of the sequences of days without precipitation. The probability of having dry spells of certain duration is estimated theoretically by employing the first-order Markov chain time series model. The probability that a dry spell will last exactly n days is given by the following analytical expression:

$$Q_n = p_{00}^{n-1}(1 - p_{00})$$

where $\mathbf{P}_{00}$ is the probability of a dry day following a dry day.

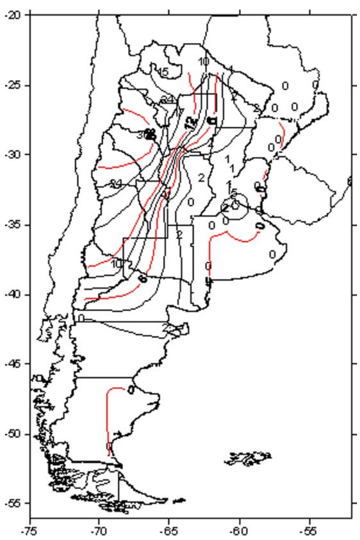

Figure 3: Number of dry spells of length equal to or more than 60 days

For further details on the theoretical distributions used, the reader is referred to Feller (1968), Katz (1974) and Wilks (1995). In order to verify the goodness-of-fit, statistics X were computed and the spatial fit variations were inspected (Buishand, 1982; Sneyers 1990). Statistics X has a X^2 distribution with γ degrees of freedom. The agreement between the fit and observations is satisfactory at the 95% level.

3. RESULTS

3.1 Geographical distribution of dry spells

Figure 2 shows the regional distribution of the longest dry spells (in days) in Argentina. The longest dry spells are recorded in western Argentina and also in the south, while the shortest ones occur in the northeast. The analysis of the longest dry spells is relevant in the analysis of droughts and their impact on society. This is the case of the maximum dry spell occurred in Pergamino (192 days) in the summer 1996/97, which caused enormous losses in the agricultural production.

In this analysis we are interested in climatic results. So, the number of dry spells of length equal to or more than 60 is compiled in Figure 3. This result shows the rainfall regime, the greatest number of dry spells in the western region decreasing towards the east and south.

Finally, the mean length of dry spells in days is calculated. Figure 4 completes the great rainfall variation in Argentina. As a general feature, we can observe that the expected length becomes larger from east to west, with remarkably low values, in relative terms, of less than or equal to 6 days, assigned to the stations located to the east of meridian 65ºW. Conversely, the rest of the country is linked to expected lengths of 10, 11 and 12 days, with a noticeably strong positive gradient, which is evident in central-western Argentina. The isohyet of 6 days divides Argentina into two: towards the east there is a region with wetter conditions and very important agricultural production and westwards, a region of deserts which is the extension of the coastal deserts of Peru and northern Chile.

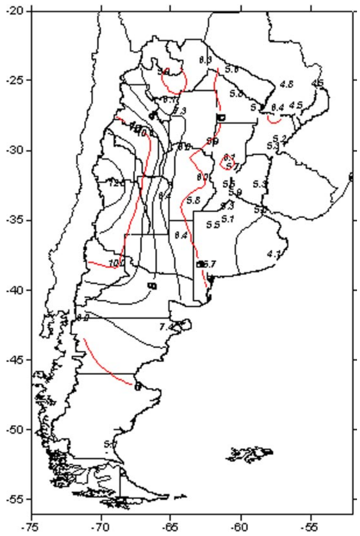

Figure 4: Mean length in days of the dry spells

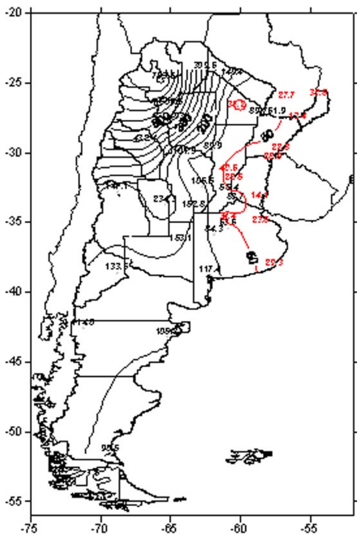

Figure 5: Empirical values of Chi-squared for each station, comparing the empirical distribution of frequencies of dry spells with the theoretical estimation using first-order Markov chain distribution models. Red figures are significant at 95%

These results show the different rainfall regime in the arid zones of Argentina. One to the east of the Andes, where the number of long dry spells has to be very high because of the summer is very dry, in contrast with the arid conditions shown in Patagonia, where the rainfall is low through the year.

3.2. Climatic frequency distributions

Upon finding the empirical distribution of dry spell frequencies according to their length, frequencies have been estimated for each station using the Markov chain distribution models. The concurrence between the fit and the series of observations is satisfactory only in the east of Argentina north of 37ºS, with a significance level of 95% (Figure 5). The biggest differences between the theoretical and empirical distribution are located in a transition zone from wet to dry episodes and in a region of dry condition.

The first–order Markov chain only takes into account the probability of a dry day following a dry day (P00). The spatial behavior of this parameter is shown in Figure 6. All the stations show high values of P00, the smallest values (0.78) appearing in the northeast. So, as the probability of a dry day after a dry day is high in a great part of Argentina, it will be difficult for a first-order Markov chain to adjust the empirical distribution.

3.3. Temporal changes in dry conditions

Atmospheric circulation in southern South America showed a significant change around the 1970´s (Agosta and Compagnucci, 2002; Barros, et al. 2000) as well as in other regions of the Southern Hemisphere (Gisbson 1992, van Loon et al 1993, Hurrel and van Loon 1994, Trenberth 1995). In order to study changes in the length of dry spells two periods are analyzed 1961–70 and 1981–90.

Figure 7 shows the spatial distribution of the average dry length (in days) for the studied area in the two periods. As a general feature, we can observe that the expected length becomes smaller in the last period. The remarkable differences are observed in the western region where the mean dry length is 11 days. It is interesting to observe that there is no evidence of change in the northeastern and eastern region and in the province of Buenos Aires.

Analogous results are obtained for the adjustment between theoretical and empirical frequencies and for the persistence P00, even though the differences between the two periods are smaller. Figure 8 shows the estimation of P00. The greater differences are again observed in the centre-west of Argentina.

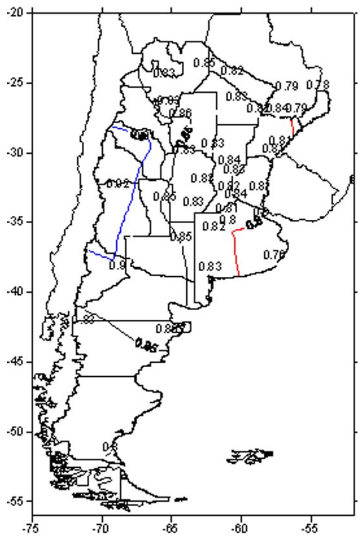

Figure 6: Persistence of no raindays

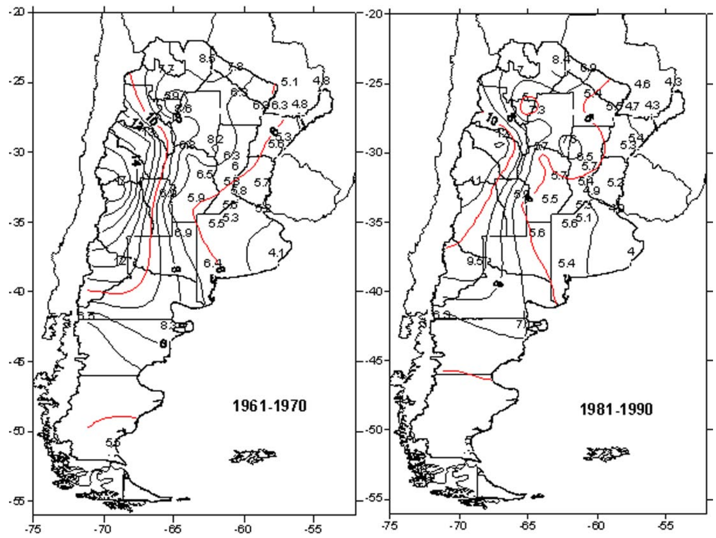

Figure 7: Mean length in days of the dry spells in two periods 1961–70 and 1981–90

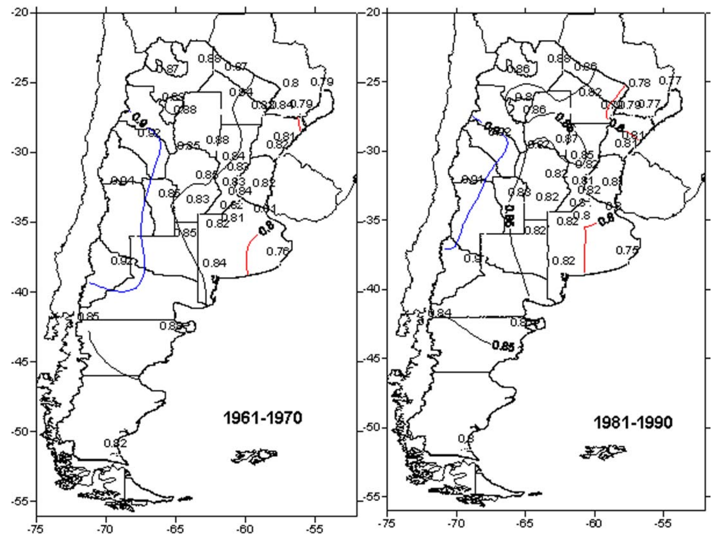

Figure 8: Persistence of no rainday in two periods 1961–70 and 1981–90

4. CONCLUSIONS

Extreme weather events in Argentina affect the agro-socio-economic environment. From the viewpoint of water resources management policy, a detailed study of drought periods is absolutely necessary as well as the forecasting of extreme episodes of consecutive dry days. The Markov chains model gives a more complete description of the behavior of dry episodes for a given rain gauge.

The length of dry spells in Argentina is very high. The mean length of the dry spells increases from east to west, from around to 5 days to more than 11 days. The longest dry spells (more than 150 days) occurred in the western region. The adjustment of the empirical distribution of frequencies of dry spells using first-order Markov chain is statistically satisfactory in northeastern Argentina. In accordance with the adjustment of the distribution of dry spells, "droughts" can be considered a Markovian process in north-eastern Argentina.

The behavior of the dry spells before and after the atmospheric circulation change around the 1970´s was analyzed. Changes are more evident in the western region. In general, the longest and mean length becomes smaller and the persistence of no rainday is less in the last period.

Acknowledgements
Support for this study was provided by the following Grants: University of Buenos Aires X135 and X234, CONICET PIP 5139 and CLARIS Project (European Commission Project 001454).

References

Buishand, T. A, 1982: Some methods for testing the homogeneit of rainfall records, J. Hydrol., 58, 11-27.
Feller, W., 1968: An Introduction to probability theory and its applications, John Willey & Sons, 509 pp.
Gregory, J.M., Wigley, T.M.L. and Jones, P.D. 1993. 'Application of Markov models to area-average daily precipitation series and interannual variability in seasonal totals', Climate Dyn., 8, 299–310.
Haan, C.T., Allen, M.D. and Street, J.O. 1976. 'A Markov chain model of daily rainfall', Water Resour. Res., 12(3), 443–449.
Katz, R.W. 1974. 'Computing probabilities associated with the Markov chain model for precipitation', J. Appl. Meteorol., 13, 953–954.
Martin-Vide J. and Gomez L, 1999: Regionalization of Peninsular Spain based on the length of dry spells, Int. J. Climatol. 19: 537–555.
Moon, S., Ryoo, S. and Kwon, J. 1994. 'A Markov chain model for daily precipitation occurrence in South Korea', Int. J. Climatol., 14, 1009–1016.
Lana X and Burgueño A, 1998: Daily dry–wet behaviour in catalonia (NE Spain) from the viewpoint of Markov Chains, Int. J. Climatol. 18: 793–815.
Penalba O., Vargas W. 2005: Low monthly rainfall in the Plata River Basin. Long term variability. Submitted to Journal of Applied Meteorology.
Penalba O.C., Robledo F. A., 2005. Frequency of precipitation in the humid pampa of Argentina, 15th Conference on Applied Climatology, 20-24 Junio 2005, Savannah, Georgia, USA.
Ruiz N., 2005: Análisis climático-estadístico de las probabilidades asociadas a condiciones secas semanales en Buenos Aires, CONGREMET IX, Buenos Aires 3-7 October 2005, Argentina
Rusticucci, M.M. and Penalba, O.C. 2000: Interdecadal changes in precipitation seasonal cycle over South America. Relationship with surface temperature. Climate Research, 16, N 1, 1-15.
Sneyers, R. 1990: On the statistical analysis of series of observations, WMO – N° 415, 192 pp.
Tolika K. and Maheras P., 2005: Spatial and temporal characteristics of wet spells in Greece Theor. Appl. Climatol. 81, 71–85 (2005)
Vargas, W.M., Alessandro, P.A.: 1985, 'Características regionales de los extremos climáticos en la región húmeda y semihúmeda argentina', Meteorológica, 15, 2, 79-92.
Vargas, W.M., Alessandro, P.A.: 1990, 'Los extremos climáticos de precipitación y temperatura en Corrientes', Meteorologica, 17, 1 y 2, 33-37.
Wilks D.F.,1995. Statistical Methods in the Atmospheric Sciences. Academic Press, 467 pp.

TRENDS IN EXTREME DAILY RAINFALL EVENTS IN LA PLATA BASIN

Olga C. Penalba, Federico A. Robledo*
University of Buenos Aires, Argentina

1. INTRODUCTION

The analysis of daily precipitation in Argentina and mainly La Plata Basin, is a subject of great interest due to the impact on agronomy and hydrology. This interest is not merely climatological; it also affects other areas of the environment and society, particularly when extreme rainfall is taken into account.

While rainfall statistics at hemisphere scale have merited attention of climatologists, regional scale rainfall still needs to be studied in order to achieve new views to describe its particular characteristics. Reasons for this include the lack of adequate data, since no climate factors (e.g. changes in station location) often bias extremes more than climatic means, and problems related with the selection of appropriate thresholds to define extremes.

Figure 1: Main orographic features of La Plata Basin

There are fewer studies of regional variability in climatic extremes in the study region. Haylock et al (2005) examine daily rainfall observations over the period 1960-2000, determining changes in both total and extreme rainfall for South America; Penalba and Vargas (2001) observed that extreme negative (positive) annual anomalies are concentrated in the first (last) half of the century in the agricultural areas of Argentina. Penalba and Robledo (2005) analyzed the annual cycle of daily percentiles and the frequency of daily rainfall events throughout the year.

Several authors have reported jumps and/or tendencies in time series of annual and seasonal rainfall in LPB, as well as in particular months or seasons of the year (Boulanger et al. 2005, Penalba and Vargas 2004 and 1996; Castañeda and Barros 1994; Rusticucci and Penalba 2000; Penalba 2004, Liebmann et al. 2004, Minetti and Vargas 1997). Moreover the isohyets in Argentina moved 200 km westward in the last century, with a positive increase specially in the humid pampas privileged the farming production (Hoffmann et al., 1987). Such discontinuities and/or trends in precipitation can affect both mean and extreme values.

The relationship between the patterns of annual and seasonal rainfall and circulation indices were analyzed by Pittock (1980) for Argentina and Chile; Barros et al.(2000) for Southern South America and Agosta and Compagnucci (2002) for central-eastern Argentina, among others. Focusing in extreme indices and sea surface temperatures we can mention Haylock et al (2005). The above-mentioned evidence shows that during the last decades significant rainfall changes occurred in some regions of the country.

In this paper, we are interested in quantifying these changes and the spatial domain. The objectives of this study are to analyze the variations in the climate indices, given by the frequency of daily precipitation and persistence; how much of the yearly index comes from each season index and a quantification of these changes and their spatial domain. Special attention is given to interdecadal and interannual variations of the climate indices, used for monitoring climate variability.

2. DATA AND METHODOLOGY

2.1 Geographic location

La Plata Basin is formed by the confluence of the Paraná and Uruguay rivers and flows to the Atlantic Ocean, and covers parts of Argentina, Brazil, Bolivia, Paraguay and Uruguay (Figure 1). The total mean annual rainfall rate in the study area is around 1200 mm. This rainfall annual quantity shows a space variation with direction NE-SW. The areas with lower annual rainfalls, approximately 300 mm, are located at the Argentinean northwest; while southern Brazil presents annual precipitations higher than 1600 mm. The mean rainfall annual cycle in the basin has a strong geographical component; varying from a very defined annual cycle (rainfall maximum during the summer) in the northern and northwestern area to a uniform seasonal distribution with maxima during spring and autumn in the eastern-central area, northeast Argentina and south of Brazil (see Penalba and Vargas, 2005 for more details). The annual cycles of daily precipitation amounts and the frequency of raindays show the same temporal variability. The persistence of raindays throughout the year shows high (low) values during the wet (drier) season. The greatest (lowest) seasonal variability is observed in the western stations (northeastern and coastal stations) (Penalba and Robledo, 2005).

2.2. Data

Long-term daily rainfall data from 34 raingauges in Argentina, located north of 37ºS and east of 67ºW, 4 raingauges in Uruguay, 10 raingauges in Brazil and 3 raingauges in Paraguay (Figure 2) were used in this study. All this information was supplied by the Argentine National Weather Service, local organizations and the databases built in the European Community Project " Assessing the impact of future climatic change on the water resources and the hydrology of the River of the Silver basin, Argentina: ARG/B7-3011/94/25".

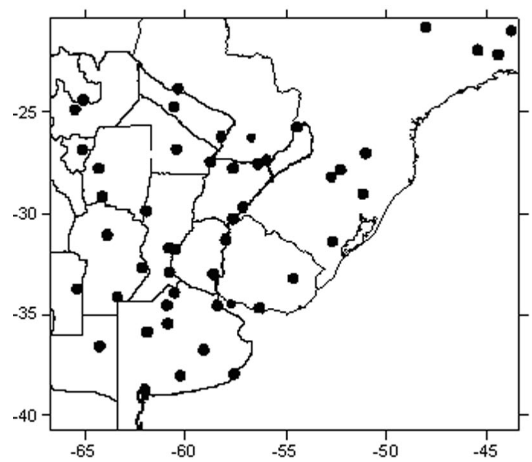

Figure 2: Distribution of the stations used in the study

The analysis of climate change indices focused on extremes requires high long records of high quality daily data. Homogeneity tests were performed (Sneyers, 1990). Only series presenting no inhomogeneities with less than 10% of missing data for their period of record were retained. The shorter period analyzed is 1972-2004 and the longest, 1908-2004.

2.3. Methodology

Extreme weather is defined by events beyond the normal range of intensity and can be identified by different thresholds in different places. Extremes of a climate variable are rarely observed events. Statistically they correspond to the far ends of the frequency distribution of the variable. Changes in extremes are, therefore, caused by changes in the frequency distribution of the variable. The indices used in this study are defined using thresholds, based on statistical quantities such as the 75th, 90th and 95th percentiles. These percentiles are clarified by smoothing the data using a 7-day running average.

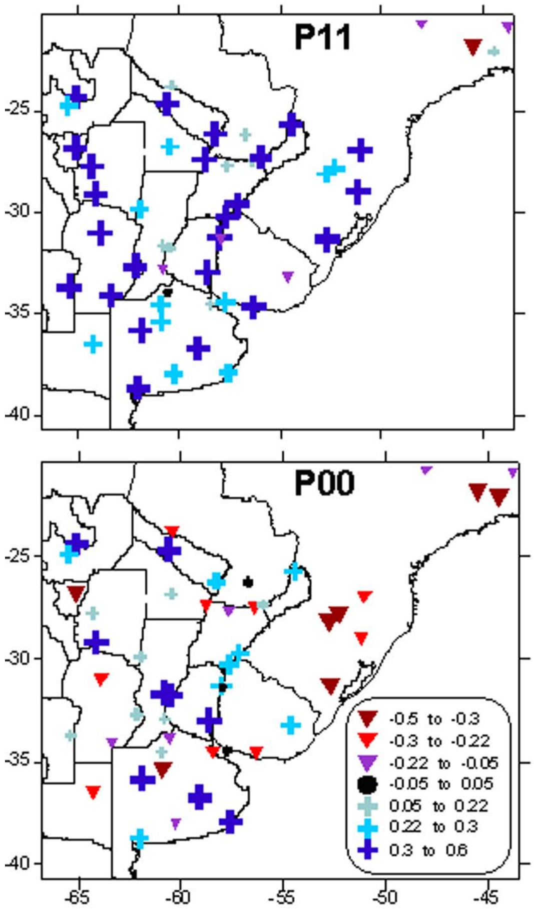

Figure 3: Sign of the trend in persistence as measured by Kendall's tau. An increase is showed by a '+', a decrease by a .'Λ' Values greater than (-0.22; + 0.22) indicate significant at p<0.05.

The aim of employing different thresholds is to detect their likely impact on the variations in the number of wet spells and their distribution. Apart from these thresholds, the selection of 0.1mm and 10 mm thresholds also has practical consequences. The former amount (0.1mm) is chosen to analyze the temporal variability of raindays and the latter (10 mm) is the rainfall amount often needed to exceed daily evaporative losses during summer months (Vargas, 1982) .

Rainfall indices were defined as:

- Persistence of raindays (no raindays): probability of rainday (no rainday) when the day before was a rainday (no rainday). Hereafter P11 and P00 respectively.
- Percentage of events: number of days with precipitation greater than or equal to 0.1, 10 mm and also their 75th, 90th and 95th percentiles of raindays (hereafter: PE > 0.1, PE > 10; PE > 75th; and so on).
- Seasonal proportion index: proportion of yearly PE index derived from seasonal PE index. Hereafter PI.

Seasonal (DJF, MAM, JJA, SON) and annual values (December to November of the next year) of these indices were calculated on a yearly basis for each station for the whole period.

Trends in the annual and seasonal indices were analyzed in a common period (1961-2000). A non-parametric Kendall Tau test was used to determine the possible existence of statistically significant trends assuming a 95% probability level (Sneyers, 1990). In this analysis the Uruguayan stations were included even when the complete period is available only at La Estanzuela station (34° 29' S and 57° 44' W).

3. RESULTS

3.1. Observed trends

To determine the most characteristic features of raindays and no raindays the temporal evolution of P11 and P00 is analyzed. Figure 3 shows the sign of the annual trends for all the stations in the common period 1961–2000. An interesting fact is the spatial coherence in sign and the significance

Table I. Number of stations with significant annual and seasonal trends

PE>0.1	DEF	MAM	JJA	SON	Annual
Negative	0	0	5	0	2
Positive	13	22	10	4	24
PE>75th	**DEF**	**MAM**	**JJA**	**SON**	**Annual**
Negative	0	0	1	1	0
Positive	7	15	1	4	19

of the annual trends of P11, showing that the probability of rainday when the day before was a rainday increases in the whole region. The probability of no rainday when the day before was a no rainday shows a greater spatial variability (Figure 3, down). Two coherence regions in sign and significance of the annual trends with opposite characteristics are observed; one in southern Brazil (negative trends) and the other over Mesopotamia region (positive trends). The signs of the trends in the rest of the region will depend on the location of the stations.

The maps in Figure 4 (left) summarize the spatial distribution of signs for the annual and seasonal PE > 0.1 trends. Almost all the stations present positive annual trends. Two large regions with spatial coherence in the significant trend are observed: one in southern Brazil and northeast

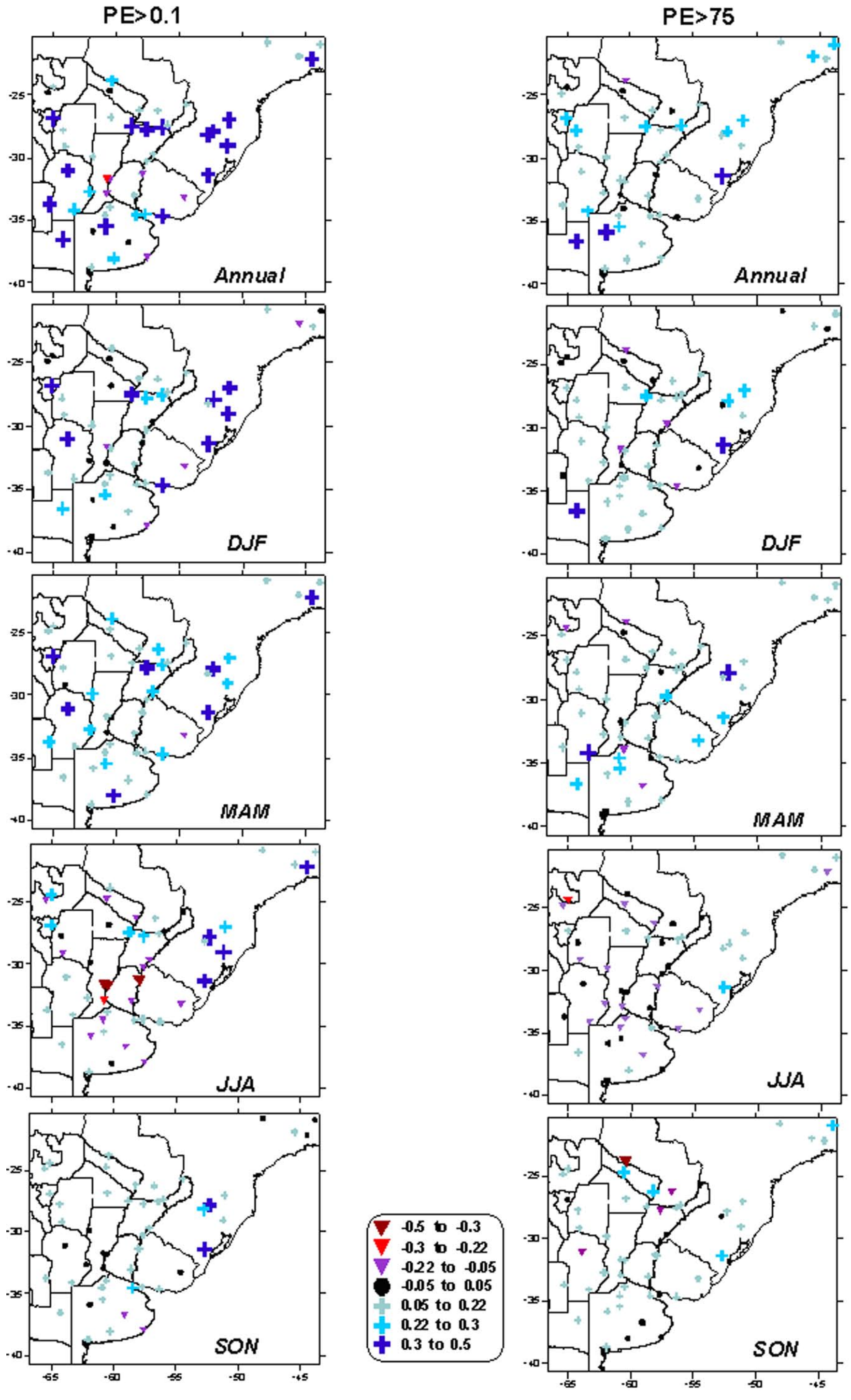

Figure 4: Idem Figure 3

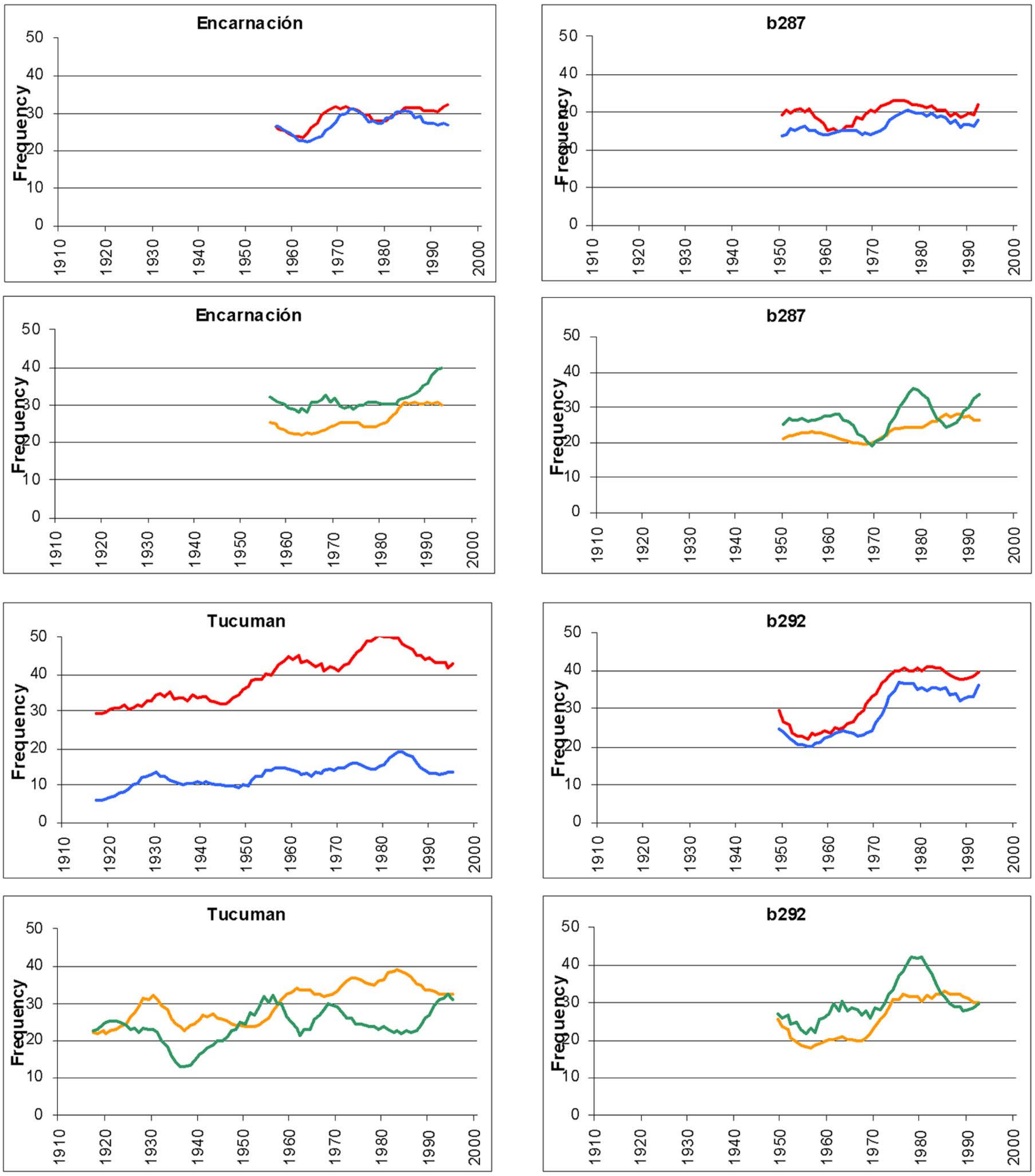

Figure 5: Time series of PE> 0.1 index for selected stations (Encarnación: -27.55, -56.38; Tucumán: -26.51, -65.12; B292: -29.03, -51.18; B287: -28.18, -52.75)

Argentina and the other in the southwest region. A small coherence region with negative annual trend is observed in the central eastern region where only one station shows significant trend. This result is mainly due to the behavior during the winter months where the negative trend is significant at some stations of this region. During these months the positive and significant trends are placed in southern Brazil and northeast Argentina. The number of stations with positive and significant trends shows seasonal variability (Figure 4, left). The seasons with the greatest values are MAM and DJF (22 and 13, respectively) and the least number of stations with significant positive trends is observed during spring months (Table I).

An important aspect of climate extremes relates to extreme droughts and moisture surpluses. We focus here on the last extreme characterized or represented by PE> 75th percentile or greater than one. The spatial pattern of the PR > 75th trends resemble the results shown before, with a de-

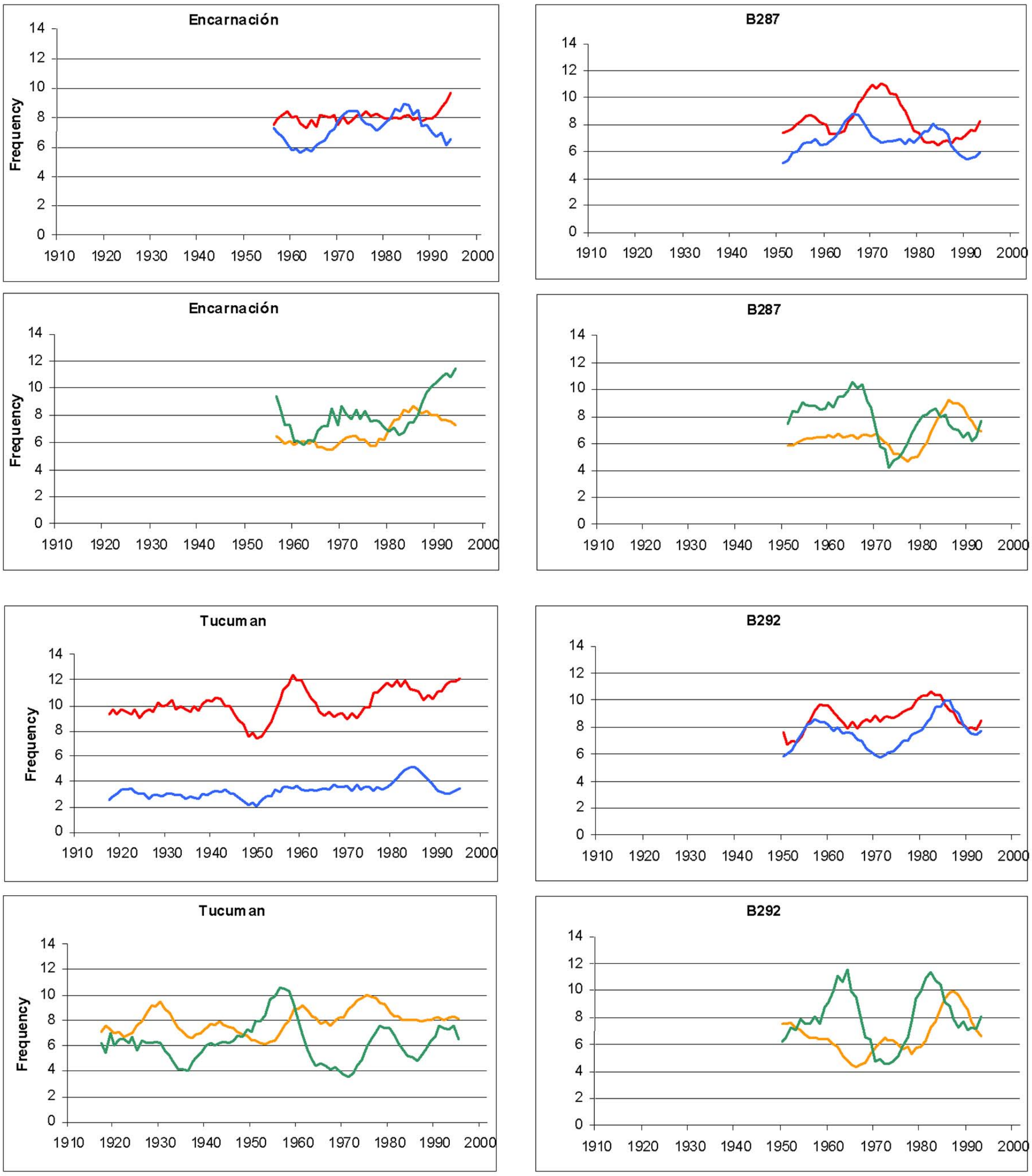

Figure 6: Idem Figure 5 for PE > 75th index

crease in the number of significant stations (Figure 4, right and Table I). In the annual index, three regions of spatial coherence in the significance of the trends are observed a) southern Brazil and northeastern Argentina; b) southwest of the study region and c) two stations in the northwest. This spatial pattern is resembled during summer and autumn months, when the index shows the greatest number of stations with significant trends (Table I).

A further examination of these indices shows different temporal behavior, depending on the season and the station. Figure 5 and Figure 6 show the time series of the seasonal values, after the 11 yr running mean was applied. The selected stations have the longest period of analysis and are located in northeast Argentina and southern Brazil, a relevant region from the hydrological standpoint. Some interannual and interdecadal variations are observed in both indices (PE>0.1 and PE>75). See for example the “maximum” values around 1975 and 1985 and the minimum around 1964 in Encarnación during JJA. The length of these periods and the central year of these maximum values will depend on the station (see JJA for B292). The longest time series analyzed are Tucumán and OCBA, located in the northwest and in the end of the Basin, respectively. The similarity between the temporal variability of the extreme index (PE>75th) and the temporal variability of PE>0.1 is interesting. See for example the two jumps in summer index around 1950 and 1970; and during spring months the minimum values around 1937 and the maximum around 1960.

The temporal variability observed in the studied indices could be due to different atmospheric and oceanographic conditions. Atmospheric circulation in Southern South America showed a significant change around 1970´s (Agosta and Compagnucci, 2002; Barros, et al. 2000) as well as in other regions of the Southern Hemisphere (Gisbson 1992, van Loon et al. 1993, Hurrel and van Loon 1994, Trenberth 1995).

The percentage changes after the 1970´s is analyzed, comparing two periods before and after this change. In order to analyze the greatest number of stations the selected periods are 1961-75 and 1980-96. Figure 7 (see cover page) shows the spatial pattern for the annual, summer and winter percentage change for PE>0.1 (left) and PE>75th (right). For both indices the greatest positive change is concentrated in a nucleus in northeast Argentina and southern Brazil. An area of relatively large values is also present in northwest Argentina with seasonal variability. The northeast of the country shows a negative change, more intense and covering a bigger area during JJA. These negative changes enhance and enlarge when the extreme index is analyzed. During spring and autumn months negative changes are only observed in small spots (not shown).

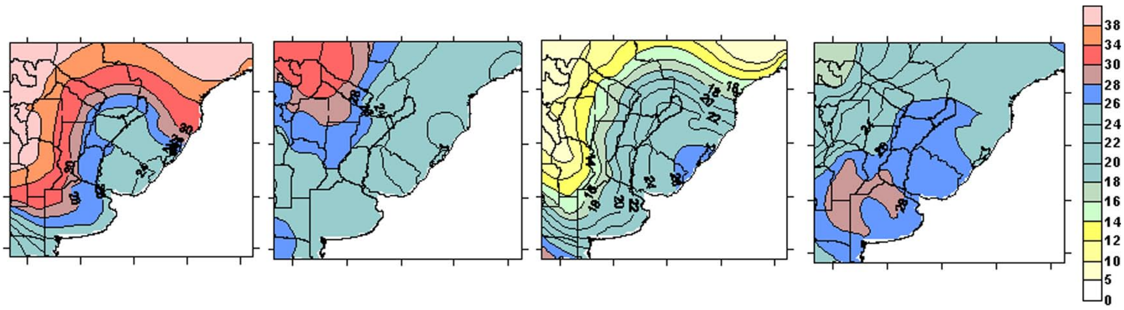

Figure 8: Seasonal proportion index for PE>75th calculated for the climatic period

3.2. Seasonal proportion index

Because changes in extreme annual indices can occur from changes in specific seasons, the seasonal proportion index is calculated.

Firstly, the climatic behavior is analyzed. The shape of the explained percentage field for each season resembles the annual cycle of the rainfall regime. Figure 8 shows the seasonal proportion index for PE>75th. During DJF months the greatest contribution is located over northwestern Argentina and the group of Brazilian stations located in the northeastern study region, decreasing towards the eastern coast of Argentina, Uruguay and south Brazil. The northwestern maximum moves towards the north of Argentina with values greater than 30% in MAM. In the rest of the region the spatial variability is low. During JJA the shape of the explained percentage field is similar to summer months, changing the gradient, minimum in the northwestern Argentina and northeast Brazil, increasing towards the eastern coast of Argentina, Uruguay and south Brazil. During SON months the greatest contribution is observed in the south, decreasing towards the northwest. This season shows the less spatial variability and winter shows the greatest one. The spatial pattern of PI for PE>0.1 indices shows similar results (not shown).

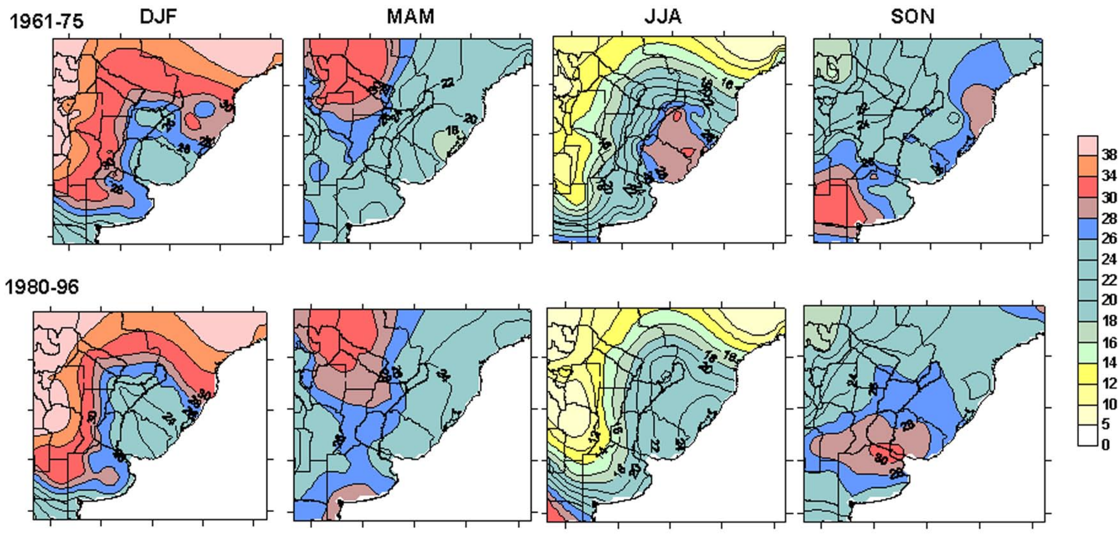

Figure 9: Seasonal proportion index for PE>75th calculated for two periods

Finally, the percentage change of PI after the 1970´s is analyzed by comparing two periods 1961-75 and 1980-96. The shape of the explained percentage field of each season resembles the long-term behavior shown in Figure 9. In the 1980-96, during DJF months the gradient increases because the maximum in the northwestern enlarge and deepen the minimum of Uruguay and south Brazil. Meanwhile during JJA months the gradient decreases, as the explained percentage is smaller over Uruguay and southern Brazil. For the transition seasons the explained percentage increases in the last period, being the mainly different located in the south close to the Río de la Plata River.

4. CONCLUSIONS

The daily rainfall regime of La Plata Basin is analyzed by means of indices given by annual and seasonal series of persistence of raindays and no raindays, number of days with rainfall greater than or equal to different thresholds; and proportion of yearly indices derived from seasonal indices.

The main objective of this paper was to analyze the trend and the temporal variability of these indices, quantifying the changes before and after the 1970's. Fifty-one stations with high quality data sets were analyzed in the longest (shorter) period 1908-2004 (1972-2004).

The hydrological consequences of accumulated precipitation falling on a number of consecutive days may be more severe than just an intense precipitation falling on a single day. The trend of PE>0.1 and PE>75th were investigated and for each season the results showed similarities and the same regions with the spatial coherence, even though the number of stations with significant trends decreases in PE>75th. There is a large region of spatial coherence in the sign of the trend, located in southern Brazil, Paraguay and northeast Argentina, showing significant increases in annual and seasonal values. Only during spring months this region conserves the sign of the trend but the number of stations with significant trends decreases. On the other hand, the winter trend was found to be the opposite for the majority of stations in central-eastern Argentina, Uruguay and few stations in the province of Buenos Aires. This result has important implications for the management of natural resources as well as for agriculture, particularly in the province of Buenos Aires where wheat production is very important. Consequently after the 1970´s, a noticeable negative change in this region was observed. As to the positive change, located in southern Brazil and northeastern Argentina, the percentage change increases in PE>75th.

The annual and seasonal trends of persistence of raindays and no raindays were also studied.

The results showed a significant positive trend in P11 in the whole region. The spatial pattern observed in P00 is remarkable. The regions with positive and negative significant trends are mainly in agreement with the results shown.

Acknowledgements
Support for carrying out this work was provided by the following Grants: University of Buenos Aires X135 and X234, CLARIS Project (European Commission Project 001454).

References
Agosta, E. A. and Compagnucci R. H., 2002: Relación entre la precipitación estival en el centro-oeste de Argentina y los campos de altura geopotencial en 1000 y 500 hpa. XXI Reunión Científica AAGG Rosario (Argentina) – 23 al 27 de Setiembre de 2002.
Barros V., Castañeda E and Doyle M., 2000: Recent Precipitation trends in Southern South America East of the Andes: An indication of climatic variability ,xxxxxxxxxxxx
Boulanger J.P., Lafon F., Penalba O., Rusticucci M., Vargas W, 2005: Observed precipitation in the Paraná-Plata hydrological basin: long-term trends, extreme conditions and ENSO teleconnections, Climate Dynamics, 24, 393-413.
Castañeda M. and V. Barros., 1994: Las tendencias de la precipitación en el cono sur de América al este de los Andes, Meteorologica XIX, 23-32.
Easterling D.R, Evans J.L, Groisman P.Y, Karl T.R, Kunkel K.E, Ambenje P. 2000. Observed variability and trends in extreme climate events: a brief review. Bulletin of the American Meteorological Society, 81: 417–425.
Haylock M. R., Peterson T., Abreu de Sousa J. R., Alves L. M., Ambrizzi T., Anunciação Y.
M. T. , Baez J., Barbosa de Brito J. I., Barros V. R., Berlato M. A., Bidegain M., Coronel G,
Corradi V., Garcia V. J., Grimm A. M.I, Jaildo dos Anjos R., Karoly D., Marengo J. A, Marino
M. B., Meira P. R., Miranda G. C., Molion L., Moncunill D. F., Nechet D., Ontaneda G.,
Quintana J., Ramirez E., Rebello E., Rusticucci M., Santos J. L., Trebejo I., Vincent L., 2005: Trends in total and extreme South American rainfall 1960-2000 and links with sea surface temperature. Accepted in Journal of Climate.
Hoffman, J.A.J., S. Nuñez and A. Gómez, 1987: Fluctuaciones de la precipitación en la Argentina, en lo que va del siglo. II Congreso Interamericano de Meteorología. Buenos Aires. Argentina.
Liebmann, B., C. S. Vera, L. M. V. Carvalho, I. Camilloni, M. P. Hoerling, V. R. Barros, J. Báez, and M. Bidegain, 2004: An observed trend in central South American Precipitation. Journal of Climate, 17, 4357-4367.
Minetti J.L. and W.M. Vargas, 1997: Trends and jumps in the annual precipitation in South America, south of the 15°S, Atmósfera, 11, 205-221.
Penalba O., 2004: Relación y variación interanual de la precipitación, frecuencia de días de lluvia e intensidad media diaria, X Reunión Argentina y IV Latinoamericana de Agrometeorología, 13 y 15 de octubre de 2004, Mar del Plata, Buenos Aires, Argentina.
Penalba, O. and Vargas W/, 2001: Propiedades de déficits y excesos de precipitación en zonas agropecuarias. Meteorologica, 26, 1 y 2, 39-55.
Penalba O., Vargas W., 2004: Interdecadal and Interannual variations of annual and extreme precipitation over central-northeastern Argentina. Changes in the extreme precipitation seasonal cycle. Int. J. Climatology, 24, 12, 1565-1580.
Penalba O.C. and Vargas W.M., 1996: Climatology of monthly and annual rainfall in Buenos Aires, Argentina. Meteorological Applications, 3, 275-282.
Penalba O., Vargas W. 2005: Low monthly rainfall in the Plata River Basin. Long term variability. Submitted to Journal of Applied Meteorology.
Penalba O.C., Robledo F. A., 2005. Frequency of precipitation in the humid pampa of Argentina, 15th Conference on Applied Climatology, 20-24 Junio 2005, Savannah, Georgia, USA.
Pittock A. B. 1980: Patterns of climatic variation in Argentina and Chile I. Precipitation. 1931-60. Mon. Weath. Rev., 108, 1347-1360.
Rusticucci, M.M. and Penalba, O.C. 2000: Interdecadal changes in precipitation seasonal cycle over South America. Relationship with surface temperature. Climate Research, 16, N 1, 1-15.
Sneyers R, 1990: On the statistical analysis of series of observation. WMO Technical Note No. 143, Geneva.
Trenberth KZ 1995. Atmospheric circulation climate change. Clim Change 31; 427-453.
Vargas, W, 1982: Atlas de Excesos y deficiencias de humedad en la región húmeda y semiárida Argentina, Tomo 2. CIBIOM.

ON THE RELATIONSHIP BETWEEN SAM AND FROST DAYS AS REPRESENTED BY AN ENSEMBLE OF IPCC AR4 MODELS

Claudio G. Menéndez (1) and Andrea F. Carril (2)

Introduction

The Southern Annular Mode (SAM) is the dominant pattern of climate variability in the southern extra-tropics. It is characterized by a meridional seesaw in atmospheric mass between Antarctica and the mid-latitudes, accompanied by an out-of phase relation in the strength of the zonal flow along 60°S and 40°S. The SAM exerts a strong influence on the extratropical climate, not only over the Southern Ocean and Antarctica (e.g. Carril et al. 2005), but over the southern continental regions as well (e.g. Silvestri and Vera, 2003).

(1) Centro de Investigaciones del Mar y la Atmósfera, CONICET/UBA, Buenos Aires, Argentina
(2) Istituto Nazionale di Geofisica e Vulcanologia, Bologna, Italy

Frich et al. (2002) defined ten indices related to extreme weather in temperature and precipitation. These "extreme indices" (annual indicators derived from daily temperature and precipitation time series) were computed by some modeling centers for climate change simulations in the framework of the IPCC Fourth Assessment Report (AR4). Meehl et al. (2005) and Tebaldi et al. (2006) provide a first overview of projected changes in climate extremes from the IPCC AR4 model ensemble. This recent literature analyses the trends in globally averaged values of extreme indices and the global spatial patterns of changes under different emissions rates. In these studies, the indices have been regarded only over continental areas.

The extent to which the SAM is linked to the extreme events is not yet clear. The SAM could shape not only the mean conditions, but also the daily variability. Consequently extreme events could be sensitive to SAM-related changes in the characteristics of extratropical storms, blocking highs and cold air outbreaks throughout the southern mid- to high latitudes. Our aim is to assess if the climate extremes provided by the AR4 coupled models are sensitive to the SAM and to examine the projections of these extremes for the end of the 21st century for the SRES A1B scenario over the Southern Ocean and embedded land areas.

For the sake of brevity, in this letter we only present results related with a particular index: the ''total number of frost days'' ("Fd" as named by Frich et al., 2002). Fd is defined as the total number of days per year with absolute minimum temperature below 0˚C. This index is particularly pertinent to the extratropical regions and it is associated with anomalies in the length of spring and fall seasons. We consider that selecting Fd is helpful as a basis to examine processes related with generating the geographic patterns of changes in temperature extremes. Other indices (including precipitation indices) will be discussed elsewhere.

Methodology

Our study is based on seven IPCC AR4 models: GFDL-CM2.0, GFDL-CM2.1, INMCM3.0, IPSL-CM4, MIROC3.2-hires, MIROC3.2-medres and MRI-CGCM2.3.2a. These models are those that had the extreme indices reported for the 20th century climate (period 1970-1999) and for the 21st century climate (SRES A1B scenario, period 2070-2099), over both continental and oceanic areas, to the Program for Climate Model Diagnosis and Intercomparison (PCMDI). Some documentation of the models is available at the PCMDI Web site (http://www-pcmdi.llnl.gov/). For our purposes, it is enough to mention that these models represent the present-day state-of-the-art in global coupled models.

Input data are annual series of geopotential height at 500 hPa and total number of frost days. The SAM is defined as the leading empirical orthogonal mode (EOF-1) obtained from 500 hPa geopotential height (Z500) anomalies, over a domain south of 42°S. The anomalies are relative to the

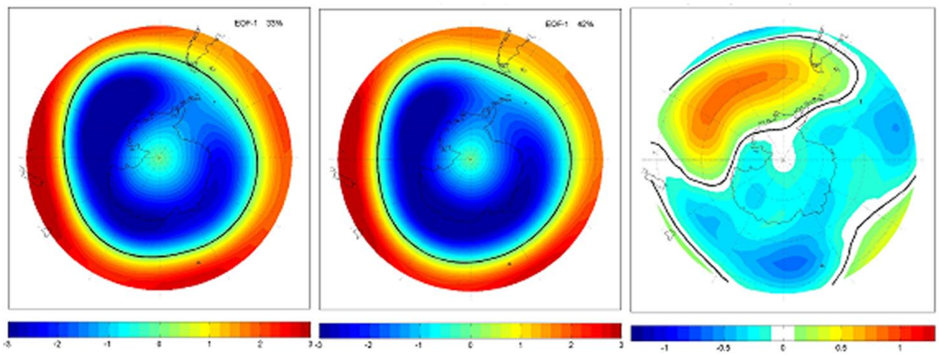

Figure 1: First EOF of annual mean Z500 anomalies for the present climate (left panel), the A1B scenario (central panel), and the difference (2070-2099 minus 1970-1999, right panel).

best straight-line fit linear trend from every single-model input data and are area weighted by the square root of cosine of latitude. We identify years during which a particular phase of the SAM is strong (years in which the principal component, PC-1, is above one standard deviation of its mean value). As when detrending, the standard deviations are also estimated model by model.

Outcomes

The SAM simulated by the ensemble of AR4 models exhibits a high spatial correlation with the observed patterns during the late 20th century, though the mode represents too large a percentage of total temporal variability (Miller et al., 2006). Both observations and simulations show a trend in the SAM towards its positive phase with decreasing sea level pressure over Antarctica and a compensating increase in midlatitudes. In response to increasing concentrations of greenhouse gases and tropospheric sulfate aerosols, the AR4 ensemble also evidences a positive annular trend, accompanied by a poleward shift of the SH storm tracks and a similar shift in the midlatitude jets and surface zonal wind stress (Yin, 2005; Russell et al., 2006).

Previous results (e.g. Carril et al., 2005) indicate that the recent rapid warming over the Antarctic Peninsula would be a consequence of the (observed and simulated) trend in the annular mode towards its positive phase. Despite the simulated positive future trend in the SAM, the pattern of the projected temperature response (not shown) is quite different from the pattern of the observed trend in recent decades. The annual mean ensemble projections show a relative uniform warming around Antarctica. In particular, the concentrated warming of the Antarctic Peninsula as compared to the rest of the continent is not predicted to continue.

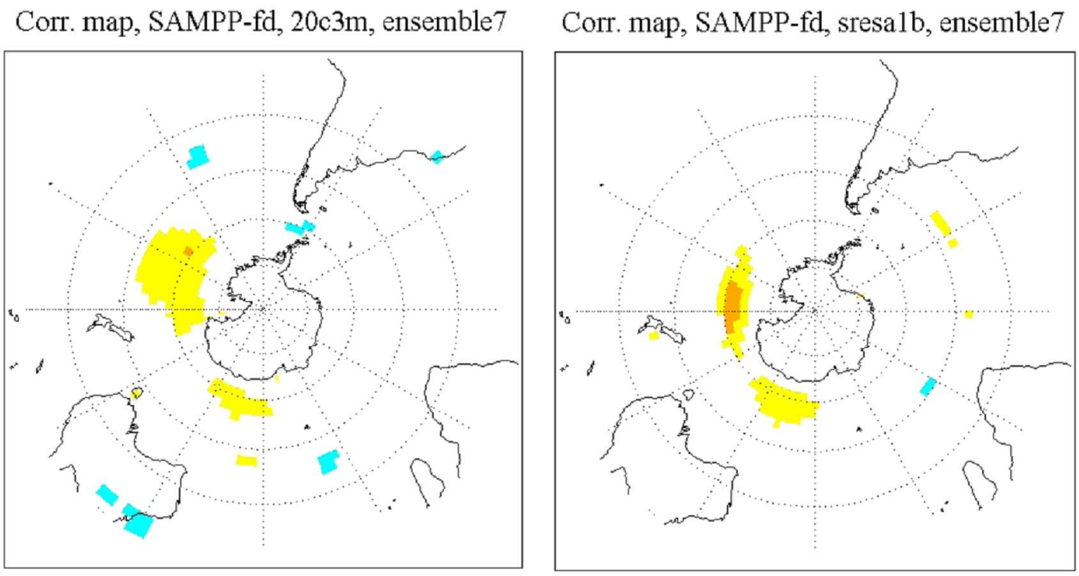

Figure 2: Spatial correlations of the annual number of frost days and the SAM for 1970-1999 (left panel) and 2070-2099 (right panel). Only significance levels for correlation values greater than 90% are shown.

Figure 1 shows the EOF-1 of annual mean Z500 anomalies for both time slices. In our multi-model ensemble, the leading mode explains 33% of the total variability during 1970-1999 and 42% during 2070-2099. In the present day time slice (left panel), the positive phase of the SAM is accompanied by large heat and humidity advections over the Antarctic Peninsula sector. The spatial pattern of the EOF-1 in the second time slice (central panel) is more zonally symmetric and, interestingly, the loadings derived from the A1B scenario are weaker in the south eastern Pacific compared to the present climate. Consequently, the poleward advection over the Antarctic Peninsula associated with the SAM positive phase tends to weaken during the late 21st century (and in contrast, it tends to increase near the Ross Sea). These large-scale atmospheric circulation changes are able to drive at least part of the simulated changes in surface temperature and in the number of frost days.

Figure 2 suggests significant correlations between variations in the SAM and variation in the number of frost days in some areas of the Southern Ocean, seemingly because changes in the SAM are associated with changes in the location and intensity of the meridional flow, as discussed in the previous paragraph. In the present climate, the Drake Passage is anticorrelated with the positive phase of the SAM (i.e., those years during which the positive phase of the SAM dominates are characterized by a small number of frost days). A contrasting behavior, with stronger correlations, is evident between 90˚E and 120˚W. Over the late 21st century, significant correlations vanish in the Drake Passage region, but are stronger to the north of the Ross Sea, consistently with the projected geographical changes in EOF-1 (fig, 1, right panel). Over the continents correlations are not significant.

The number of frost days during years with strong positive phase compared to years with strong negative phase shows a clear regional contrast between the Drake Passage region and the rest of the Southern Ocean (fig. 3, left panel). The multimodel ensemble qualitatively agrees with the observed pattern for the recent decades of the 20th century of a reduced severity in temperature minima over the Antarctic Peninsula region associated with the trend in the SAM toward its high-index polarity. Over South America, the number of frost days during the present climate seems to be related to the SAM along the Andes between about 20˚S and 40˚S and over central Argentina, with more frost days occurring when positive phase dominates. Associated with general increases of temperatures, in the future climate the number of frost days diminish almost everywhere, and consistently the magnitude of the differences in Fd between the positive and negative phases of the SAM is reduced (fig.3, right panel). In particular, this pattern shows almost no change in frost days in the positive phase compared to the negative phase in the Drake Passage and Weddell Sea. Finally, note that southern Patagonia is a region that shows a decrease in frost days associated with the positive phase of the SAM during both time slices.

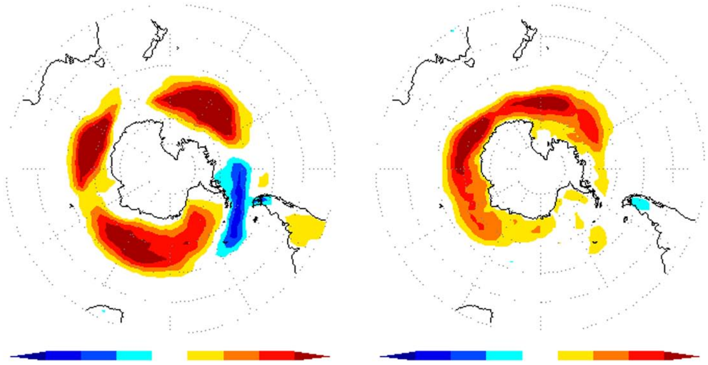

Figure 3: Composite patterns of Fd (days) during years with strong SAM positive phase minus Fd during years with strong SAM negative phase for 1970-1999 (left panel) and 2070-2099 (right panel)

Final remarks

The main interest of this research relies on the influence of the SAM on extreme weather events in the southern extratropics. In this preliminary study, we have documented some aspects of an extreme temperature indicator (the number of frost days) as simulated by a subset of the AR4 models. In particular, we have illustrated its association with the SAM and its response to climate change, as these are critically important aspects for understanding climate trends and projections in the southern extratropics. Our results highlight the fact that, though there is a general decrease in the number of frost days with global warming, the changes in regional atmospheric circulation associated with the SAM certainly influence the pattern of changes in this extreme index. However, other several interrelated physical processes not analysed here (e.g. feedbacks with soil moisture over land or with sea ice over ocean), could also contribute to the pattern of changes in the number of frost days.

Acknowledgments

We acknowledge the international modeling groups for providing their data for analysis, the Program for Climate Model Diagnosis and Intercomparison (PCMDI) for collecting and archiving the model data, the JSC/CLIVAR Working Group on Coupled Modelling (WGCM) and their Coupled Model Intercomparison Project (CMIP) and Climate Simulation Panel for organizing the model data analysis activity, and the IPCC WG1 TSU for technical support. The IPCC Data Archive at Lawrence Livermore National Laboratory is supported by the Office of Science, U.S. Department of Energy. This research was done in the framework of CLARIS EU project. A. F. Carril was partially supported by CLARIS (GOCE-CT-2003-01454) and by MERSEA IP project (SIP3-CT-2003-502885) and C.G. Menéndez by project PIP 5416 (CONICET, Argentina).

References

Carril A.F., C.G. Menéndez, and A. Navarra, 2005: Climate response associated with the Southern Annular Mode in the surroundings of Antartic Peninsula: A multimodel ensemble analysis. Geophy. Res. Lett., 32, L16713, doi:10.1029/2005GL023581.
Meehl G.A., Arblaster J.M., and Claudia Tebaldi, 2005: Understanding future patterns of increased precipitation intensity in climate model simulations. Geophys. Res. Lett., 32, L18719, doi:10.1029/2005GL023680.
Miller R.L., Schmidt G.A., and Shindell D.T., 2006: Forced annular variations in the 20th century Intergovernmental Panel on Climate Change Fourth Assessment Report models. J. Geophy. Res., 111, doi:10.1029/2005JD006323.
Russel J.L., R.J. Stouffer, and K.W. Dixon, 2006: Intercomparison of the Southern Ocean circulation in IPCC coupled model controm simulations. J. Clim. 19 4560-4575.
Silvestri G.E. and C.S. Vera, 2003: Antarctic Oscillation signal on precipitation anomalies over southeastern South America. Geophys. Res. Lett., 30(21), doi:10.1029/2003GL018277.
Tebaldi, C., K. Hayhoe, J.M. Arblaster, and G.E. Meehl, 2006: Going to the extremes: an intercomparison of model-simulated historical and future changes in extreme events. Climatic Change, 79, 185-211, doi: 10.1007/s10584-006-9051-4.
Yin J.H., 2005: A consistent poleward shift of the storm tracks in simulations of 21st century climate. Geophys. Res. Lett., 32, L18701, doi:10.1029/2005GL023684.

SIMULATED SKIN TEMPERATURE OUTLOOK

Rafael Terra
Instituto de Mecánica de los Fluidos e Ingeniería Ambiental
Universidad de la República, Uruguay

Quality of climate simulations largely depends on the models ability to capture the evolution of the slower components of the climate system (ocean, land-vegetation, ice) and how those affect the atmospheric circulation on the region of study. Without attempting to describe the evolution of these coupled climate subsystems in any detail, we present a brief outlook of model simulated skin temperature, a variable that directly affects atmospheric forcing. Results for the CLARIS partner's models IPSL's CM4 (Madec et al., 1999), MPI's ECHAM5/OM (Roeckner et. al, 2003) and INGV's SXG (ECHAM4.6/OPA8.2 –Gualdi et al. 2003) are presented for two hundred-year runs: 20C (1901-2000) and sresA1B scenario (2001-2100).

Given that El Niño – Southern Oscillation (ENSO) is a dominant mode of climate variability in the globe and its influence on Southeastern South America is well known, some emphasis is placed in describing the evolution of simulated Niño 3 Index for current and future climates.

1. 20th Century Simulations

Skin temperature (SKT) annual cycle for each model is shown for the period 1970 to 1999. Figures 1, 2 and 3 present each model's climatology as compared to the HadISST data set (Rayner et al., 2003).

There are several features in the biases that are common to all models. The trades region on the western and equatorward flank of subtropical anticyclone, upwind the region dominated by stratocumulus, tend to be too warm. This warm bias spreads basin-wide in the Atlantic Ocean, accentuating the northward meridional temperature gradient in the subtropical South Atlantic, most predominantly in the IPSL simulations.

In the equatorial Pacific, on the other hand, models' behavior diverges. IPSL model shows a warm bias (reflected also on Niño 3 Index – Fig 4.) especially on the western half of the basin, therefore reducing the longitudinal temperature gradient. MPI model presents a too strong cold tongue and a greater amplitude on the El Niño 3 annual cycle associated to the exaggerated interannual variability shown by this model (Table 1). Figure 4 shows the annual cycle for Niño 3 Index, synthesizing the observed and simulated climatology of the central equatorial Pacific where ENSO develops. Contrary to the MPI model, INGV and IPSL seasonal cycle in the equatorial Pacific is somewhat weaker than observed.

Table 1 shows the standard deviation and dominant frequencies in the observed and simulated Niño 3 indices. Singular

Table 1: Standard Deviation and dominant periodicities (as determined by SSA) of observed and simulated Niño 3 Index for the period 1901-2000

	Standard Deviation	Dominant Cycles (% Variance Explained)		
Observed	0.91 ˚C	4.5 yrs (25%)	3.3 yrs (20%)	
MPI	1.45 ˚C	5.5 yrs (30%)	3.0 yrs (24%)	1.9 yrs (7%)
IPSL	1.04 ˚C	4.2 yrs (13%)	3.2 yrs (16%)	2.3 yrs (36%)
INGV	0.91 ˚C	4.6 yrs (32%)	3.3 yrs (14%)	2.5 yrs (18%)

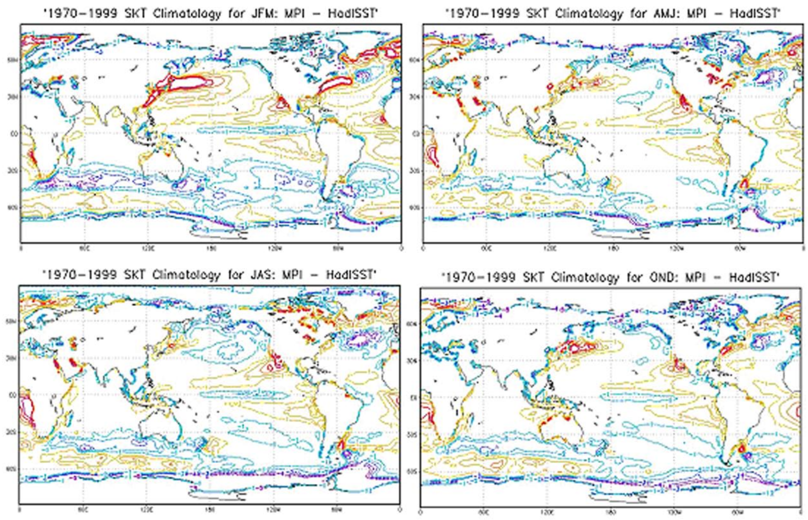

Figure 1: Seasonal cycle of simulated MPI SKT for the period 1970-1999 as compared with HadISST dataset (MPI-HadISST)

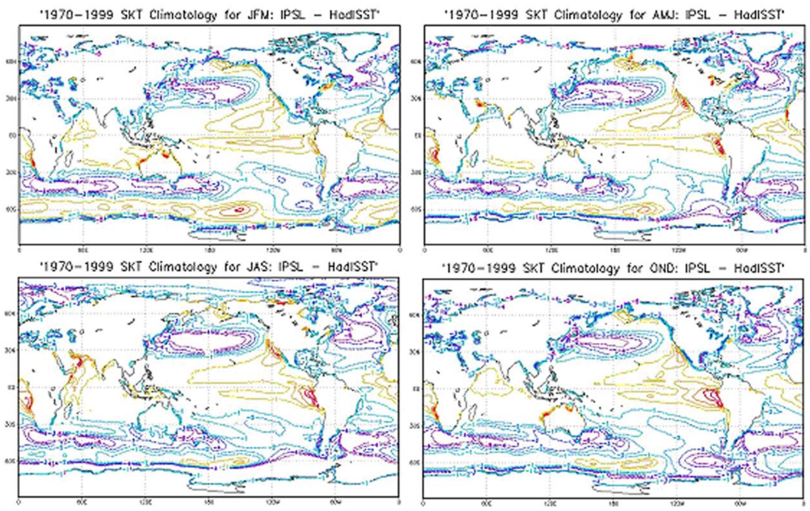

Figure 2: Seasonal cycle of simulated IPSL SKT the period 1970-1999 as compared with HadISST dataset (MPI-HadISST)

Spectral Analysis –SSA- (Ghil et al. 2002) was performed to each time series after removing the respective annual cycles. A 120 months (10 year) window was used targeting those frequencies typical of ENSO. We only show the periodicity and explained variance of the significant (and marginally significant) quasi-oscillations as determined by Monte Carlo analyses. It is worth noting that none of the series showed a statistically significant trend component. MPI model shows too strong ENSO-related variability, a feature that must be kept in mind when analyzing the simulated teleconnections with regions where ENSO has a strong influence, like Southeastern South America. IPSL-simulated ENSO is too bi-annual, the 2.3 years cycle is the most dominant, while variance in the 3-5 years band is weaker than observed. The INGV model, on the other hand, shows a remarkably realistic variability in the Niño 3 Index, both intensity and dominant frequencies.

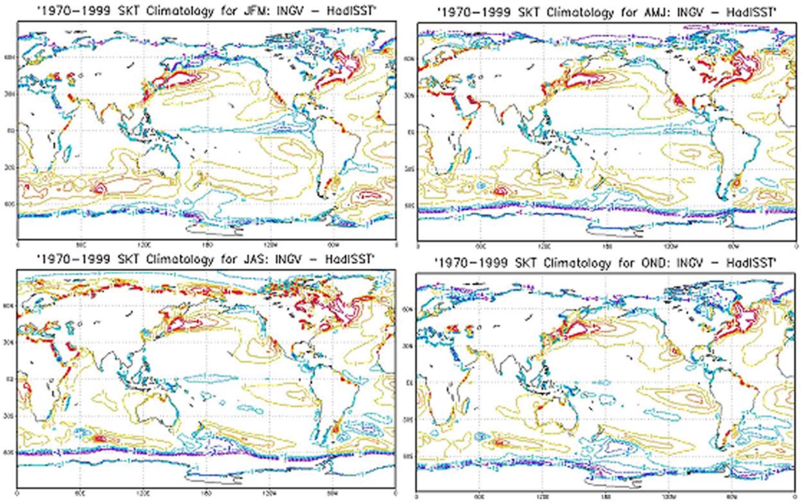

Figure 3: Seasonal cycle of simulated INGV SKT the period 1970-1999 as compared with HadISST dataset (MPI-HadISST)

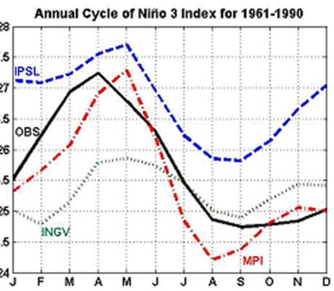

Figure 4: Annual cycle of Niño 3 Index for the period 1961-1990: Observed (solid), MPI model (dot-dashed), IPSL model (dashed) and INGV model (dotted)

2. Scenario sresA1B

The climatology of each model for the period 2071-2100 of sresA1B scenario is presented as compared to the respective model climatology for 1970-1999. Figures 5, 6 and 7 show the annual cycle of the difference between those time-periods for each model.

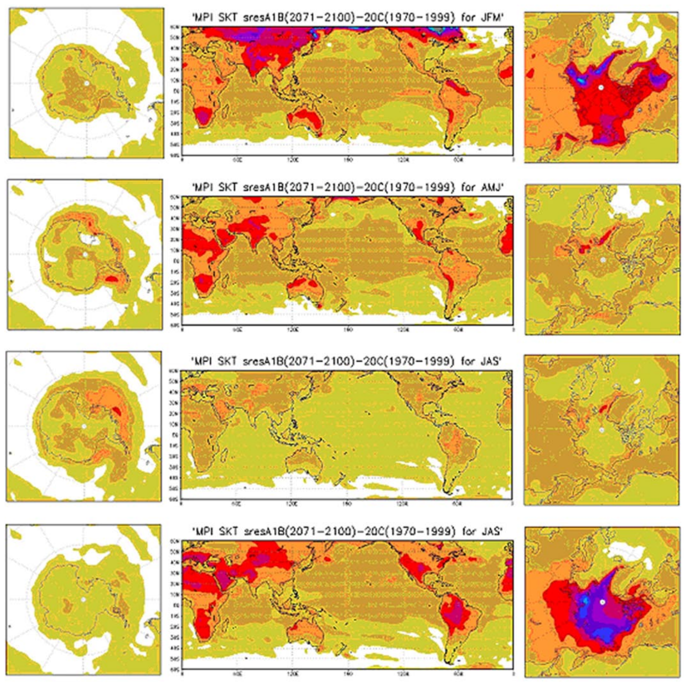

Figure 5: Seasonal cycle of simulated MPI Skin Temperature warming for the period 1971-2000 (sresA1B scenario) as compared to 1970-1999. Shading starts above +1ºC or below -1ºC for all panels and changes every 1ºC (2ºC) at the central (lateral) panels

All panels in Figures 5, 6 and 7 show the typical signature of global warming with highest warming in high latitude cold season, especially in the Northern Hemisphere. Warming in the tropical ocean is between 2 to 3 degrees in most cases and weaker in the North Atlantic and the Southern Oceans. We make no attempt to analyze these patterns in any detail. However, we do point out an interesting difference between MPI and INGV models on one side and IPSL model on the other regarding warming patterns over the South American continent, which directly concerns the regional climate. In the MPI and INGV models, the pattern of skin temperature warming over the continent is centered on the Equator, more intensely during the second half of the year, especially in the MPI case where amplitude reaches up to 6˚C in JAS. In the first half of the year the pattern is weaker and reflects that of the surrounding oceans. In contrast, the IPSL model shows a well-defined subtropical (off-equatorial) maximum in skin temperature warming over Southeastern South America with some seasonal variation in latitude. Although there are some differences in the surrounding SST among models, this feature suggests a different behavior of land-atmosphere feedbacks among models. Further analysis of precipitation and low level moisture convergence performed for different regions of South America within CLARIS may build up on these results.

Next we show the annual cycle for Niño 3 Index for the period 2070-2100, sresA1B scenario (Figure 8) and the difference

Table 2: Standard Deviation and dominant periodicities (as determined by SSA) of simulated Niño 3 Index for the period 2000-2100 (sresA1B scenario)

	Standard Deviation	Dominant Cycles (% Variance Explained)		
MPI	1.85 ˚C	Trend (29%)		
Detrended	1.51 ˚C	3.8 yrs (37%)	2.6 yrs (16%)	2.0 yrs (9%)
IPSL	1.27 ˚C	Trend (40%)		
Detrended	0.95 ˚C	4.1 yrs (10%)	3.1 yrs (13%)	2.2 yrs (28%) 1.9 yrs (18%)
INGV	1.10 ˚C	Trend (40%)		
Detrended	0.83 ˚C	5.2 yrs (31%)	2.7 yrs (13%)	2.0 yrs (12%) 1.8 yrs (10%)

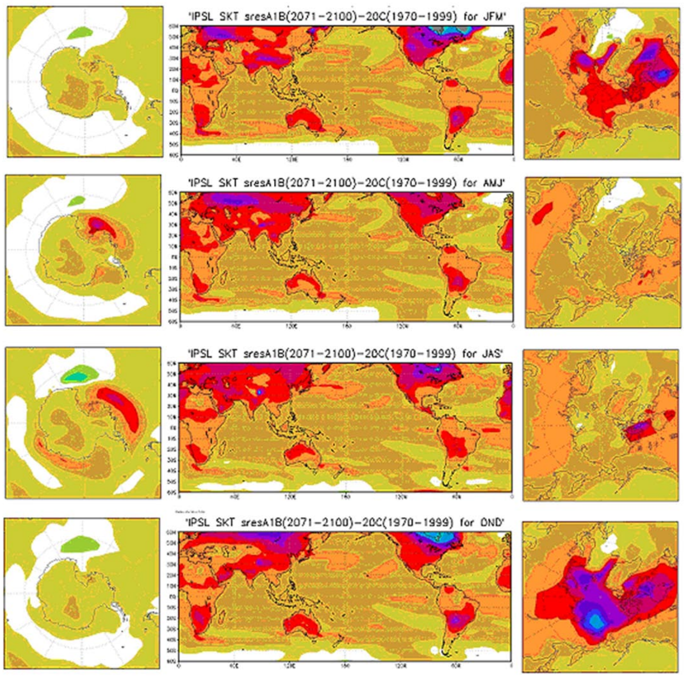

Figure 6: Seasonal cycle of simulated IPSL Skin Temperature warming for the period 1971-2000 (sresA1B scenario) as compared to 1970-1999. Shading starts above +1ºC or below -1ºC for all panels and changes every 1ºC (2ºC) at the central (lateral) panels

References

Ghil M., R. M. Allen, M. D. Dettinger, K. Ide, D. Kondrashov, M. E. Mann, A. Robertson, A. Saunders, Y. Tian, F. Varadi, y P. Yiou, 2002: Advanced spectral methods for climatic time series, Rev. Geophys., 40(1), 1003, doi:10.1029/2000RG000092.
Gualdi, S., A. Navarra, E. Guilyardi, and P. Delecluse 2003: Assessment of the tropical Indo- Pacific climate in the SINTEX CGCM, Ann. Geophys., 46, 1 – 26.
Madec, G., P. Delecluse, M. Imbard, and C. Levy, 1999: OPA 8.1 Ocean General Circulation Model reference manual, Internal Rep. 11, Inst. Pierre-Simon Laplace, Paris, France.
Rayner, N.A., Parker, D.E., Horton, E.B., Folland, C.K., Alexander, L.V, Rowell, D.P., Kent, E.C. and Kaplan, A., 2003: Globally complete analyses of sea surface temperature, sea ice and night marine air temperature, 1871-2000. J. Geophysical Research 108, 4407, doi:10.1029/2002JD002670
Roeckner et. al, 2003: The atmospheric general circulation model ECHAM5 Report No. 349OM.

with the 1971-2000 climatology (Figure 9) for each model. Mean warming is approximately 2.7˚C for both MPI and IPSL models and 2.3˚C for INGV. Therefore, models mostly maintain the relative difference shown for the 20th century. However, seasonal distribution of the warming is model dependant, it tends to smooth the already weak IPSL annual cycle (rendering it even weaker) and tends to accentuate it in the INGV and MPI simulations.

As in Section 1, each model's annual cycle was removed from the time series and interannual variability was examined through SSA. Not surprisingly, a trend component dominates in all cases as it is shown in Table 2. The reconstructed time series associated with the trend component is shown in Figure 10. SSA was repeated after subtracting the trend component to the original time-series. In the MPI and IPSL models, the standard deviation of the detrended Niño 3 time series is slightly higher than for the 20th century, while for the INGV model it is slightly smaller.

With several minor shifts in the frequencies and explained variance, the dominant cycles of each model resemble the ones obtained for the 20th century simulation. In summary, ENSO statistics do not seem to be substantially altered in the sresA1B scenario beyond the emergence of notorious trend. This is not to say that the impact of ENSO in a particular region may not be modified due to climate warming.

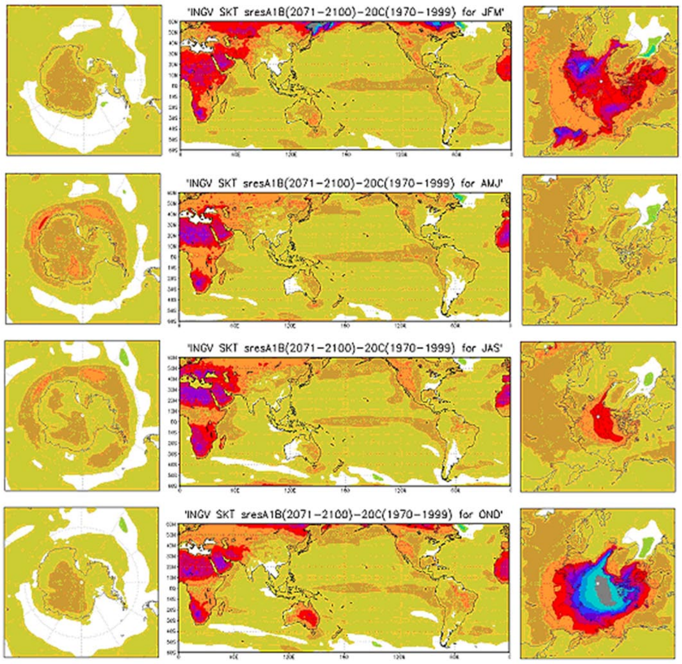

Figure 7: Seasonal cycle of simulated INGV Skin Temperature warming for the period 1971-2000 (sresA1B scenario) as compared to 1970-1999. Shading starts above +1ºC or below -1ºC for all panels and changes every 1ºC (2ºC) at the central (lateral) panels

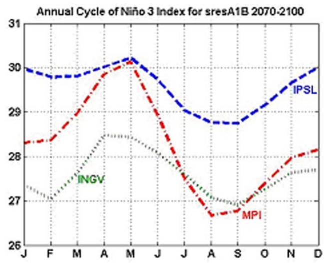

Figure 8: Annual cycle of Niño 3 Index for the period 2071-2100 (sresA1B scenario.) MPI model (dot-dashed), IPSL model (dashed) and INGV model (dotted)

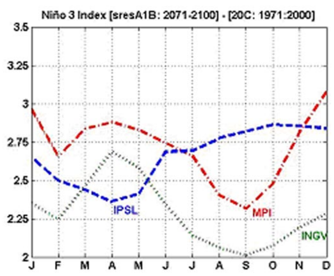

Figure 9: Annual cycle of simulated Niño 3 Index warming for 2071-2100 (sresA1B) compared to 1961-1990 period. MPI model (dot-dashed), IPSL model (dashed) and INGV model (dotted)

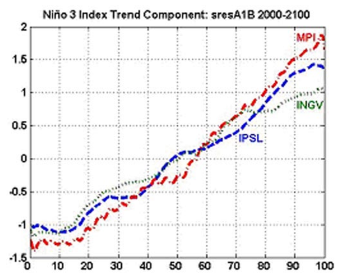

Figure 10: Trend component in simulated Niño 3 Index for 200-2100 period (sresA1B scenario.) MPI model (dot-dashed), IPSL model (dashed) and INGV model (dotted)

INFLUENCE OF SOIL MOISTURE INITIAL CONDITIONS ON SOUTH AMERICAN MONSOON DEVELOPMENT

Anna A. Sörensson, Claudio G. Menéndez
Centro de Investigaciones del Mar y la Atmósfera, CONICET-UBA, Buenos Aires, Argentina
Patrick Samuelsson, Ulf Hansson, Ulrika Willén, Markku Rummukainen
Rossby Centre, Swedish Meteorological and Hydrological Institute, Norrköping, Sweden

Introduction

The South American Monsoon System (SAMS, Nogués-Paegle et al., 2002) dominates the mean seasonal cycle of precipitation in tropical and subtropical latitudes. The timing of its onset and duration and the frequency and intensity of daily rainfall have important implications for many climate studies and water resources management applications. The soil moisture memory could influence the development of the SAMS and potentially contributes to atmospheric variability and seasonal predictability. The purpose of this ongoing study is to analyze the sensitivity of the monsoon precipitation to late (austral) winter soil moisture initial conditions on the daily and intraseasonal timescales simulated by the Rossby Centre regional atmospheric climate model RCA3 (Kjellström et al., 2005; see also http://www.smhi.se/sgn0106/if/rc/rca.htm).

Anomalous soil moisture conditions affect the near-surface climate through modified energy flows, thus the atmospheric stability is altered and may so have an impact on precipitation (Pielke, 2001). Altered rainfall affects soil moisture. However, this feedback should not be thought of as merely positive (e.g. dry conditions generate dryer conditions), but as a complex and geography-dependent feedback process. For example, Beljaars et al. (1996) found that soil moisture anomalies were associated to non-local precipitation anomalies. Soil moisture – precipitation feedback processes is an issue that has not been fully addressed in South America yet.

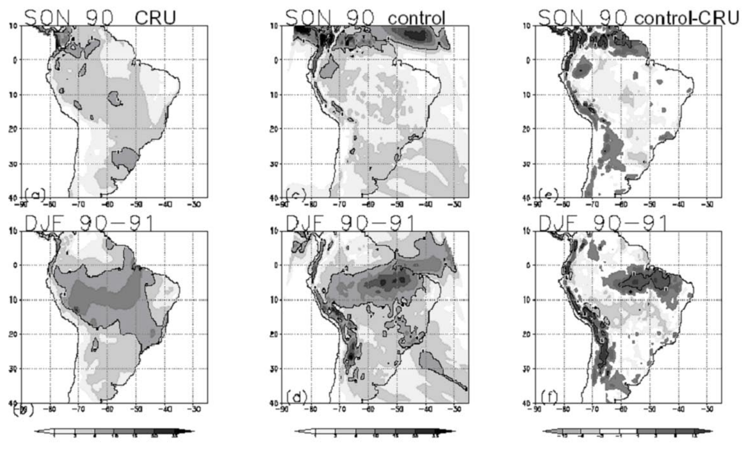

Figure 1: Seasonal precipitation for CRU (a, b), control (c, d) and control minus CRU (e, f). Contour line at 6 mm/day

Two recent sensitivity studies performed with regional models have explored the effects of initial soil moisture on precipitation, focusing on particular years and areas. Ferreira et al. (2006) performed 10-days simulations over South America with WRF for January 2003. They found that dry surface conditions increased sensible heat and near-surface temperature, producing a deeper Northwestern Argentinean Low. The local precipitation was also reduced. Collini et al. (2006) carried out a one-year-long simulation with the Eta model and showed that dry conditions reduced the evaporation and that the moisture transported by the South American low level jet was reduced.

Three recent works discuss the relation between SAMS and the land surface. Xue et al. (2006) study the role of vegetation biophysical processes in the structure and evolution of SAMS through GCM experiments with different land surface parameterizations. They show that the simulation of SAMS improves when using parameterizations that include an explicit representation of vegetation processes (e.g. radiative transfer in the canopy, water interception loss and canopy transpiration) in the calculation of surface fluxes. Fu and Li (2004) and Li and Fu (2004) discuss the relative importance of the land surface conditions for the onset of the SAMS using ERA15 data. They find that the continental surface conditions seem to control the onset date of the monsoon, in particular that a dry land surface could delay the onset of SAMS with as much as two months.

We performed three simulations of the period 1 September 1990–30 April 1991 using a continental scale domain nested in reanalysis data. Two of them have modified initial soil moisture, with anomalously dry and wet land surface conditions over the whole domain, and will in the following be called “D” and “W” respectively. The initial soil water availability (SWA) was taken from the driving reanalysis, in this case ERA40. The SWAERA40 was multiplied by a factor 0.2 to generate dry conditions, and we used the formula SWAWET=SWAERA40 + (1- SWAERA40)*0.8 to generate wet conditions. The “control” simulation was initialized without modifying the initial soil moisture.

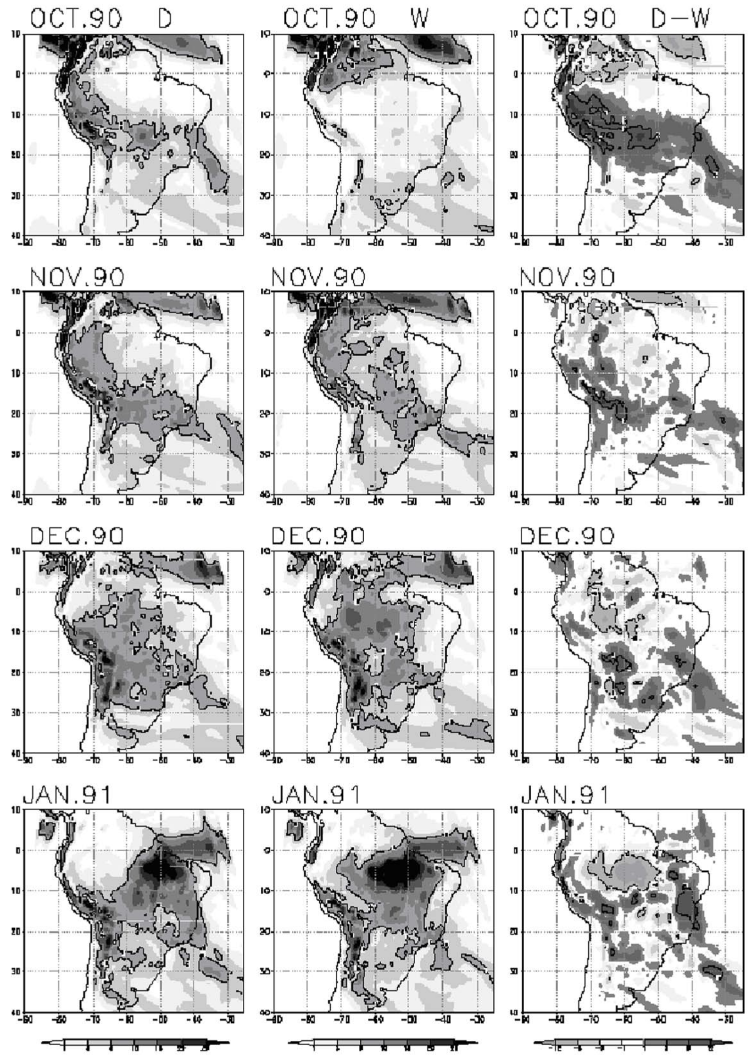

Figure 2: Monthly precipitation for October through January (mm/day) for dry (left column), wet (middle column) and dry-wet (right column). Grey shading levels are 1, 3, 6, 10, 15, 20 and 25 mm/day (left and middle columns) and ±1, ±3, ±6, ±12 mm/day (right column). The line 6 mm/day is highlighted

Results

Figure 1 shows the September-November (SON) and December–February (DJF) mean precipitation from CRU (left panels), control simulation (middle panels) and the model biases (control minus CRU, right panels). The simulated precipitation during SON is weak in the monsoon region and in southern Brazil, but the model is too wet in the region affected by the ITCZ (northern South America) and in the exit region of the South American low level jet (northern Argentina). During the austral summer, the monsoon precipitation was simulated, including the South Atlantic Convergence Zone (SACZ), albeit western Amazon along the Andes was dry and eastern Amazon was too wet. In addition, the control experiment exhibited too much precipitation along the eastern slopes of Central Andes, as well as large areas of light precipitation in parts of south eastern South America. Some of these deficiencies have been found in a number of simulations for South America performed with global and regional models.

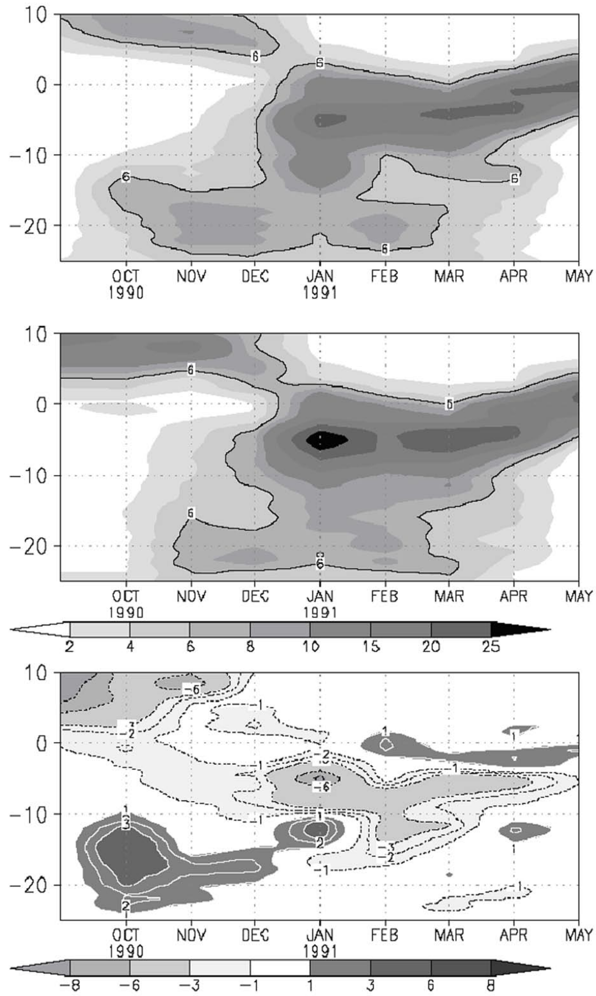

Figure 3: Temporal evolution of the monthly mean precipitation (mm/day) averaged over 40°–60°W from September through May: dry (upper panel), wet (middle), and dry minus wet (bottom). Vertical axis shows latitudes

Figure 2 shows the monthly mean precipitation for the D and W experiments in the period October through January, which were the crucial months for development of the SAMS. Regions of intense rain (more than 6 mm day–1) are highlighted. This is a complex system with land surface–atmosphere interactions depending on numerous factors. The figure suggests that the soil moisture initial condition has a strong influence on wet season rainfall over the continental convective monsoon regions. However, a wetter (dryer) land surface does not always coincide

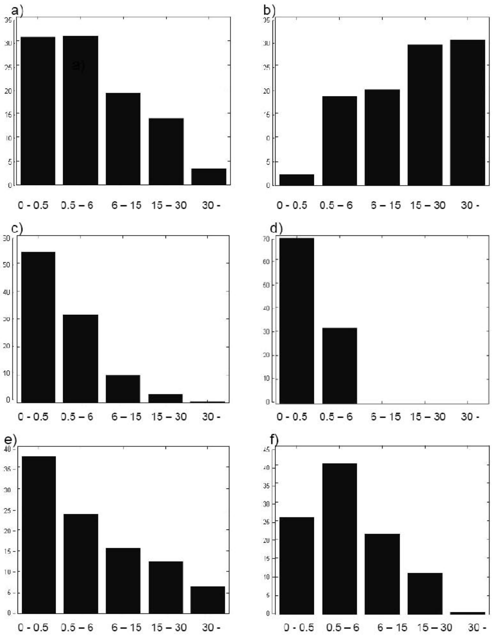

Figure 4: Histograms of daily January precipitation rates (mm/day) over Amazonia (3°S–8°S, 63°W-53°W) (a, b), central-eastern Brazil (14°S-20°S, 44°W-40°W) (c, d), and northern Argentina (24°S-28°S, 62°W-58°W) (e, f), for the dry (left panels) and wet (right panels) experiments (ordinate in percentage)

with more (less) evaporation and precipitation. In the comparison D-W, some areas are drier where the monsoon either was delayed or could not reach any further development, and others are wetter due to redistribution of the circulation or changes in position of the maximum precipitation band. The changes of land surface conditions also affected the precipitation over ocean due to the impact of land–atmosphere interaction on circulation, similar to Sato et al. (1989) and Xue et al. (2006). Compared to experiment D, experiment W increases precipitation along the ITCZ especially in the development phase of SAMS (October-November). Compensating subsidence produce large areas of decreased precipitation further south in tropical South America. During the mature phase of monsoon development (December-January), experiment W enhances rainfall in Amazonia. The region of maximum precipitation extends toward the southeast and the South Atlantic (i.e. the SACZ). Experiment W tends to produce a SACZ shifted southward and increased rainfall over large areas of subtropical South America.

To outline more clearly the premonsoon and monsoon evolution during the rainy season, we illustrate in figure 3 the monthly mean precipitation, zonally averaged between 60°W and 40°W, from September through May. The development phase of SAMS during austral spring of 1990 was characterized by the presence of the ITCZ in the northern part of the domain; with a tendency toward moving southward especially in experiment D. A strong precipitation band between 15°S and 25°S appears from October in experiment D and one month later in experiment W. Meanwhile, the rapid southward shift of the region of intense convection from the equator toward the southern Amazon Basin is manifested earlier in experiment W (in November). During the mature phase, rainfall intensity is heavier in case W over the SAMS core region, but case D simulates stronger precipitation further south over eastern Brazil and the nearby Atlantic. The decay phase continues through austral summer as convection gradually retreats northward toward the equator merging with the ITCZ. The band with intense precipitation is stronger in experiment W, but tends to be wider (more meridionally extended) in experiment D.

In order to provide a more detailed picture of the model's sensitivity than the monthly mean values, figure 4 displays the histograms of daily rainfall over three continental areas where January sensitivity is particularly strong: Amazonia, central-eastern Brazil and northern Argentina (monthly mean rainfall decreases in Amazonia and increases in the other two regions in experiment D). The methodology is to count for each grid point, the total number of days within each interval representing dry days (0-0.5 mm/day) and light (0.5–6 mm/day), moderate (6–15 mm/day), strong (15–30 mm/day) and heavy (> 30 mm/day) precipitation days. Such a diagnostic of simulated rainfall on a daily basis must be considered with caution taken into account that only one month within a single seasonal-long case study is analyzed.

The soil moisture late winter initial conditions have a strong effect on the frequency distribution of the daily rainfall rates in January. This effect is regionally dependent, but over these three regions, the distribution of the simulated precipitation rates shows significant differences. Over Amazonia, dry surface initial conditions tend to drastically decrease the number of intense convective rainstorms (i.e. strong and heavy rainfall days) and the number of wet days. Over central-eastern Brazil dry days are less frequent in experiment D, but experiment W does not favor the occurrence of rainfall rates exceeding 6 mm/day. Northern Argentina shows an increased number of both dry days and heavy rainfall days as a response to decreased initial soil moisture.

Obtaining a better understanding of the effect of land surface conditions on the SAMS development and the associated daily rainfall characterization is useful for various research areas, including seasonal forecasting and climate change studies. Of course, studying the impact of soil moisture initial conditions constitutes a limited approach as part of the difficulty for understanding and simulating the hydrologic cycle in this region. In this simple and qualitative assessment of the soil–precipitation feedback, we have analyzed seasonal-long simulations with opposite soil moisture initial conditions in order to represent two highly idealized and extreme anomalous surface conditions during the late austral winter. Our results suggest that the initial springtime soil moisture conditions feed back upon the SAMS during the warm months, not only over Amazonia but in subtropical South America as well.

Acknowledgements: This work was begun while A.A Sörensson visited Swedish Meteorological and Hydrological Institute (SMHI) in Norköping, Sweden, invited by Rossby Centre and with financial support from SMHI and CLARIS (www.claris-eu.org). We acknowledge National Supercomputer Center in Linköping, Sweden, where the simulations were carried out on Tornado. A.A. Sörensson has a grant from Rossby Centre, SMHI. PIP/CONICET 5416 (Argentina) also supported this work.

References

Beljaars, A.C.M., P. Viterbo, M. Miller, and A.K. Betts, 1996: The anomalous rainfall over the USA during July 1993: Sensitivity to land surface parametrization and soil moisture anomalies. Mon. Wea. Rev., 124, 362-383.

Collini, E. A., E. H. Berbery, and V. Barros. 2006. Seasonal dependence of surface-atmosphere interactions for subtropical South America. Proceedings of the 8th ICSHMO, Foz do Iguaçu, Brazil, April 24-28, 999-1004.

Ferreira, L.J., C. Saulo, J. Ruiz, and M. Seluchi, 2006: The impact of land use changes over the low level circulation related to the Northwestern Argentinean Low. Proceedings of the 8th ICSHMO, Foz do Iguaçu, Brazil, Apr.24-28, 1029-1035.

Fu.R and W. Li, 2004: The influence of the land surface on the transition from the dry to wet season in Amazonia, Theoretical and Applied Climatology, 78, 97-110.

Kjellström, E., Bärring, L., Gollvik, S., Hansson, U., Jones, C., Samuelsson, P., Rummukainen, M., Ullerstig, A., Willén U. and Wyser, K., 2005. A 140-year simulation of European climate with the new version of the Rossby Centre regional atmospheric climate model (RCA3), Reports Meteorology and Climatology No. 108, SMHI, SE-60176 Norrköping, Sweden, 54pp.

Li. W. and R. Fu, 2004: Transition of the Large-Scale Atmospheric and Land Surface Conditions from the Dry to the Wet Season over Amazonia as Diagnosed by the ECMWF Re-Analysis. J. Clim., 17, 2637–2651.

Nogués-Paegle J., and co-authors, 2002: Progress in Pan American CLIVAR research: understanding the South American monsoon. Meteorologica, 27, 1-30.

Pielke, R.A. Sr., 2001: Influence of the spatial distribution of vegetation and soils on the prediction of cumulus convective rainfall. Rev. Geophysics, 39, 151-177.

Sato, N., P. J. Sellers, D. A. Randall, E. K. Schneider, J. Shukla, J. L. Kinter III, Y.-T. Hou, and E. Albertazzi, 1989: Effects of implementing the simple biosphere model in a general circulation model. J. Atmos. Sci., 46, 2757–2782.

Xue Y., F. J. Zeng, K. E. Mitchell, Z. Janjic and E. Rogers. 2001: The Impact of Land Surface Processes on Simulations of the U.S. Hydrological Cycle: A Case Study of the 1993 Flood Using the SSiB Land Surface Model in the NCEP Eta Regional Model. Mon. Wea. Rev., Vol. 129, No. 12, pp. 2833–2860.

CONTENTS

CLARIS News is published every six months by the CLARIS Project and distributed freely upon request.

CLARIS
c/o Departamento de Ciencias de la Atmosfera - UBA
Pabellón II - 2do piso - Ciudad Universitaria
1428 Buenos Aires - ARGENTINA
Tel: 54 11 4576 3356 or 54 11 4576 3364 ext 20
Fax: 54 11 4576 3356 or 54 11 4576 3364 ext 20
E-mail: clarisproject@cima.fcen.uba.ar
Web site: www.claris-eu.org